

LMS Durham Symposium: Computational methods for wave propagation in direct scattering. 15-25 July 2002, Durham, UK

**The *hp* version of the Weighted Regularization Method
for Maxwell Equations**

Martin COSTABEL & Monique DAUGE

Institut de Recherche MATHématique de Rennes

<http://www.maths.univ-rennes1.fr/~costabel>

References

Theory and analysis of the h -version:

M. Costabel, M. Dauge: Weighted regularization of Maxwell equations in polyhedral domains. *Numer. Math.* Online publication DOI 10.1007/s002110100388 (2002)

Numerical tests, including hp version, benchmark problems:

<http://www.maths.univ-rennes1.fr/~dauge/benchmax.html>

Numerical results in 2D:

M. Costabel, M. Dauge, D. Martin, G. Vial: Weighted regularization of Maxwell equations – computations in curvilinear polygons. *Proceedings of ENUMATH01* (2001)

Our Finite Element package:

D. Martin: Mélina.

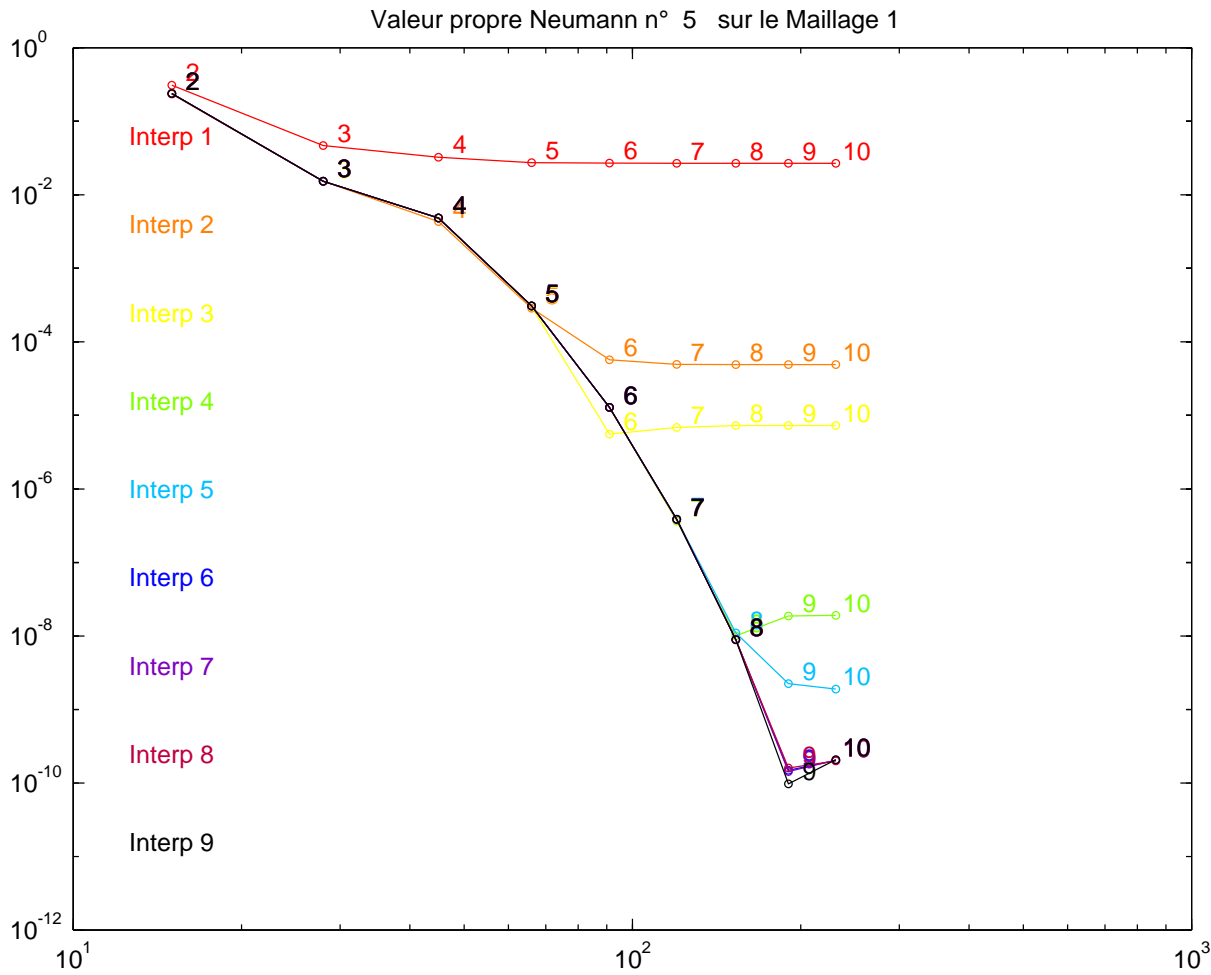
Online documentation: <http://www.maths.univ-rennes1.fr/~dmartin>

Analysis of the hp version:

M. Costabel, M. Dauge, Ch. Schwab: Exponential convergence of the hp -FEM for the weighted regularization of Maxwell equations in polygonal domains. *In preparation*

Convergence of Eigenvalues:

The Ideal...



Relative error vs # DOF

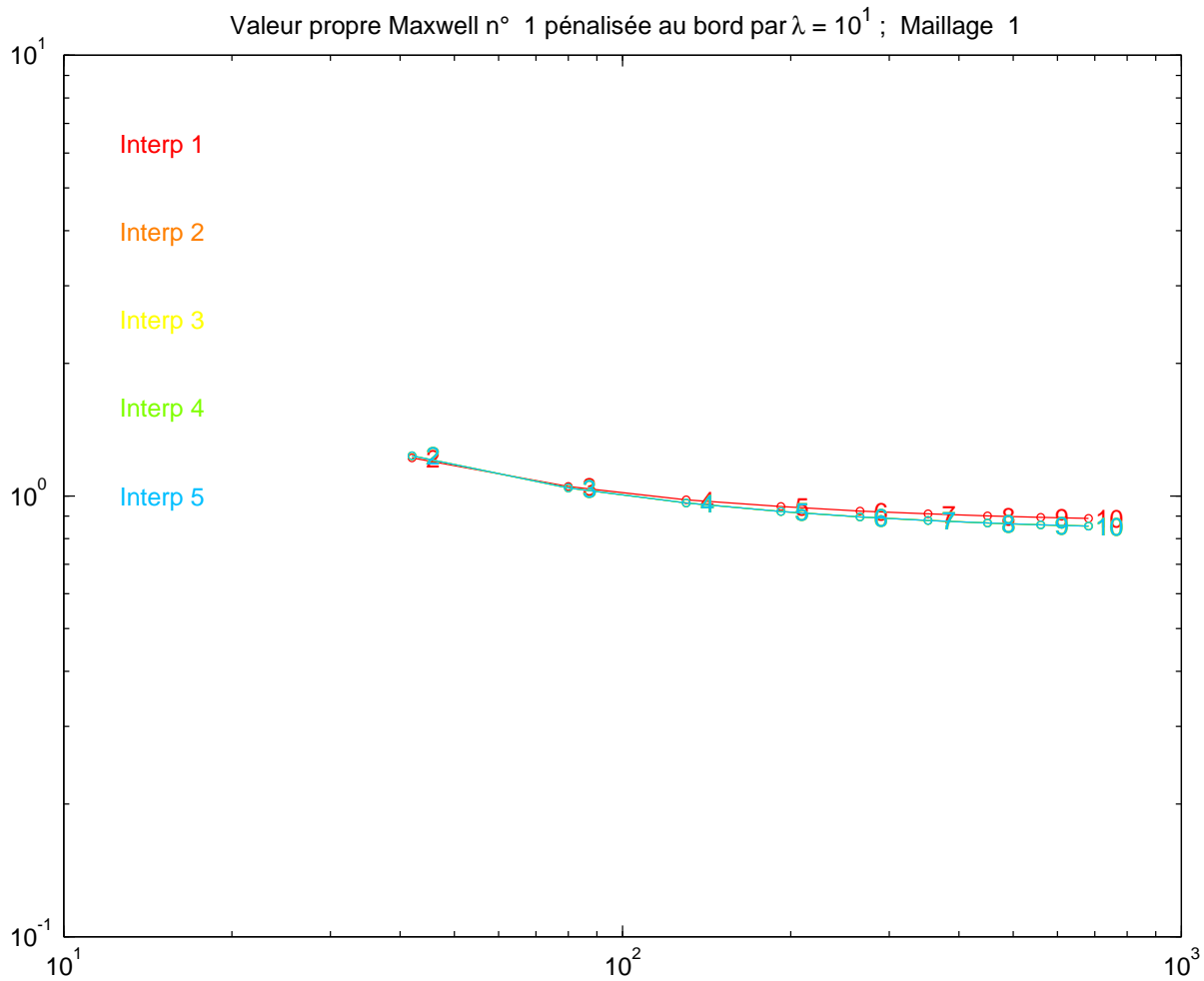
**1st Neumann
eigenvalue on a
curved rectangle**

Nodal elements

Two elements

p version

... and the reality



Relative error vs # DOF

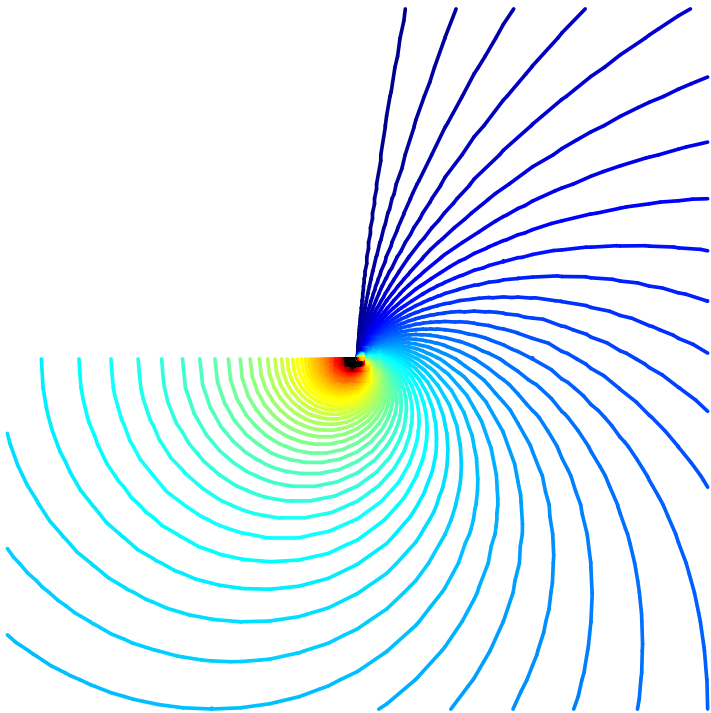
1st Maxwell
eigenvalue on a
curved L shape

Nodal elements

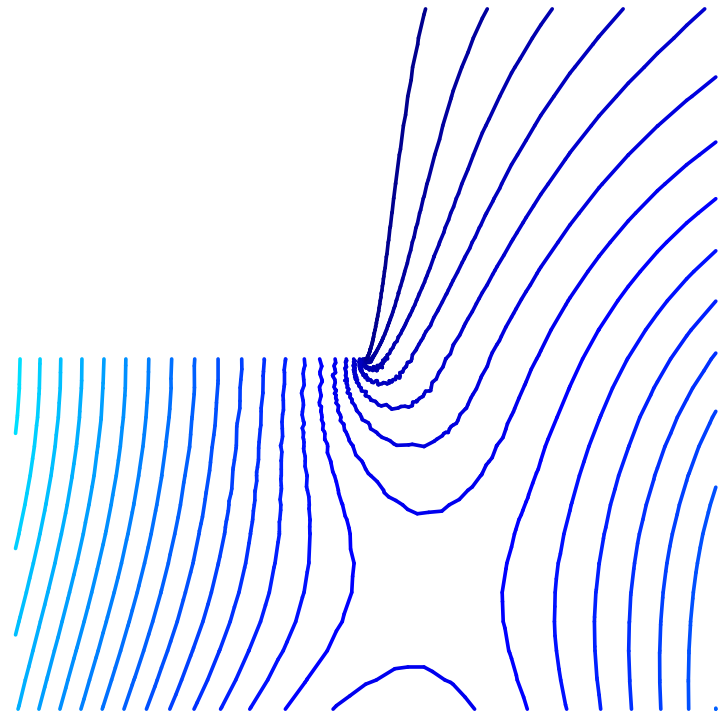
Regularization
without weight

The standard nodal “approximation” of the first singularity

The exact solution $(\text{grad}(r^{\frac{2}{3}} \sin \frac{2\theta}{3}))_1$.

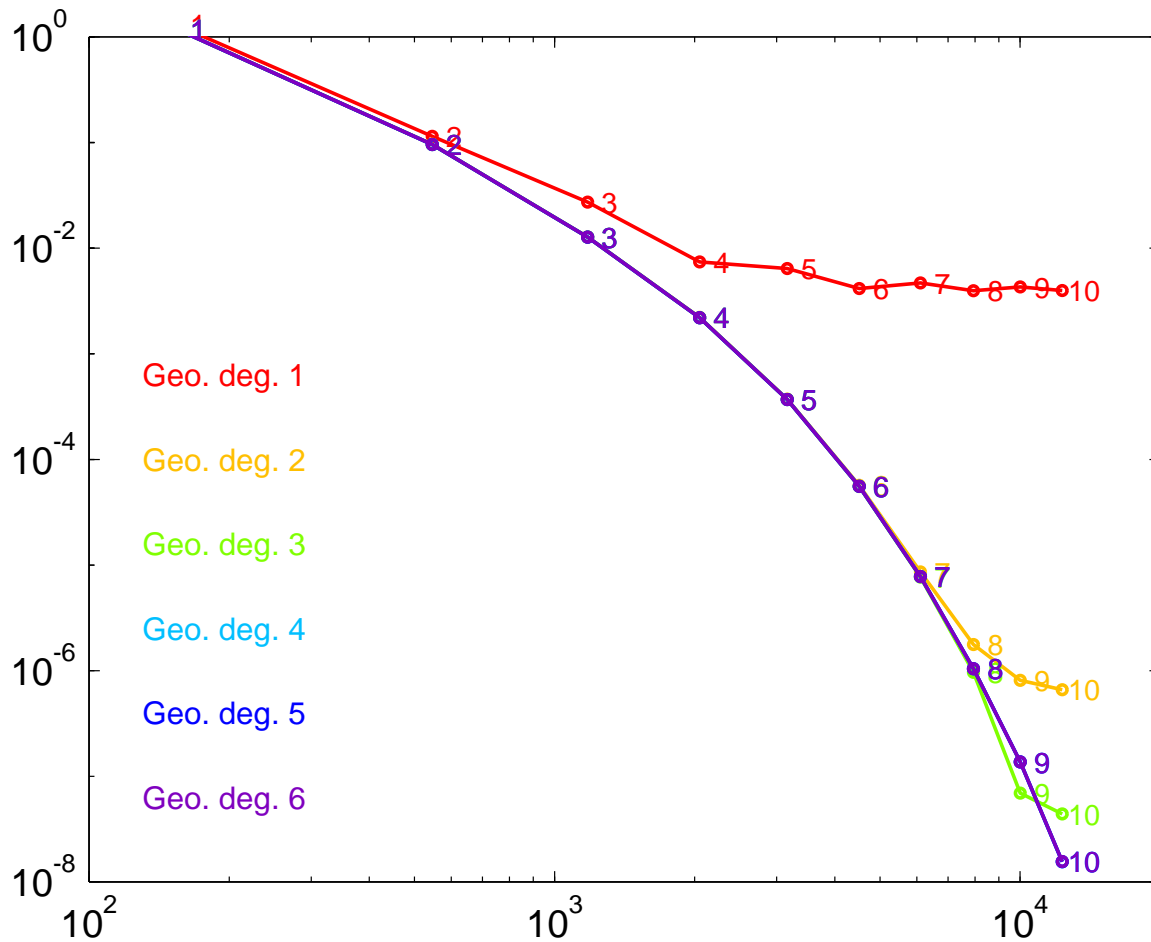


Computation with \mathbb{Q}_3 elements,
regularization without weight.



Non- H^1 singularities are not approximated.

The Ideal Recovered



Relative error vs # DOF

1st Maxwell
eigenvalue on a
curved L shape

Nodal elements

Weighted
regularization

Outline

- **The Maxwell source problem and eigenproblem and their variational formulation with weighted regularization.**
- **Convergence analysis of the weighted regularization method:**
 - The h version
 - The hp version
- **Numerical results in 2D:**
 - Straight L-shaped domain
 - Curved L-shaped domain
 - Evidence for exponential convergence
- **Numerical results in 3D:**
 - The “thick L”
 - Fichera’s corner.

Maxwell source problem

Permittivity ε and permeability μ set to 1. Ω polyhedron in \mathbb{R}^3 (or polygon in \mathbb{R}^2).

Given $\omega \in \mathbb{R}$, $J \in L^2(\Omega)^3$ with $\operatorname{div} J = 0$, find $(E, H) \in L^2(\Omega)^6$ such that

$$\text{(Maxwell SP)} \quad \begin{cases} \operatorname{curl} E - i\omega H = 0 & \& \operatorname{curl} H + i\omega E = J \text{ in } \Omega, \\ E \times n = 0 & \& H \cdot n = 0 \text{ on } \partial\Omega \end{cases}$$

Maxwell eigenvalue problem

Find non-zero ω such that $\exists (E, H) \neq 0$

$$\text{(Maxwell EVP)} \quad \begin{cases} \operatorname{curl} E - i\omega H = 0 & \& \operatorname{curl} H + i\omega E = 0 \text{ in } \Omega, \\ E \times n = 0 & \& H \cdot n = 0 \text{ on } \partial\Omega \end{cases}$$

In both cases, $\operatorname{div} E = \operatorname{div} B = 0$ is implied if $\omega \neq 0$.

Variational formulation: The WRM

Bilinear form for $s > 0$, $0 < \alpha \leq 2$,

$$a_s(u, v) = \int_{\Omega} \operatorname{curl} u \operatorname{curl} v + s \int_{\Omega} r^{\alpha} \operatorname{div} u \operatorname{div} v,$$

where $r(x) \sim \operatorname{dist}(x, \{\text{nonconvex edges and corners}\})$.

$$\text{Find } u \in \mathfrak{X} \text{ such that } \forall v \in \mathfrak{X}: a_s(u, v) - \omega^2 \int_{\Omega} u v = \int_{\Omega} f v$$

(SP): ω, f given, u unknown; (EVP): $f = 0$; $u \neq 0, \omega$ unknown.

Energy space

$$\mathfrak{X} = X_N^{\gamma} := H_0(\operatorname{curl}) \cap \{u \in L^2(\Omega)^3, r^{\gamma} \operatorname{div} u \in L^2(\Omega)\}.$$

with $\gamma = \alpha/2$.

Recall:

$$\sigma(\mathfrak{P}_{r^{\gamma}}^{[s]}) = \sigma(\mathfrak{M}) \cup s \sigma(L_{r^{\gamma}}^{\operatorname{Dir}}).$$

Galerkin approximation: Everything standard here

With the test and trial subspace $\mathfrak{X}_h \subset \mathfrak{X}$, the **Galerkin solution** $u_h \in \mathfrak{X}_h$ is defined by

$$\forall v_h \in \mathfrak{X}_h : \quad a_s(u_h, v_h) - \omega^2 \int_{\Omega} u_h v_h = \int_{\Omega} f v_h$$

Since $a_s(\cdot, \cdot)$ is positive definite and symmetric, we have the usual stability and error estimates, in particular:

- **Céa's lemma:** For the source problem and $\omega = 0$:

$$\|u - u_h\|_{X_N^\gamma} \leq \inf\{\|u - v_h\|_{X_N^\gamma} \mid v_h \in \mathfrak{X}_h\}$$

- **Convergence of the eigenvalues:** For the eigenvalue problem, $f = 0$:

Suppose $\{\mathfrak{X}_h\}_{h>0}$ is a family of subspaces approximating \mathfrak{X} .

If $\omega \in \sigma(\mathfrak{P}_{r^\gamma}^{[s]})$ is a simple eigenvalue, then there is a simple eigenvalue ω_h of the discrete problem such that

$$|\omega - \omega_h| = O((\text{energy norm error})^2).$$

The rest is approximation theory...

Birman-Solomyak decompositions

Basic idea for the estimate of the approximation error:

1. **Decomposition of the solution** $u = w + \text{grad } \varphi$, with w “regular” and φ carrying the main corner singularities

Energy norm: $\|u\|_{X_N^\gamma} \leq \|w\|_{H^1} + \|\text{grad } \varphi\|_{L^2} + \|r^\gamma \Delta \varphi\|_{L^2}$

2. **Approximation of** $u = w + \text{grad } \varphi$ **by** $u_h = w_h + \text{grad } \varphi_h$,

$$\|u - u_h\|_{X_N^\gamma} \leq \|w - w_h\|_{H^1} + \|\varphi - \varphi_h\|_{V_\gamma^2},$$

where $w_h \in \mathfrak{X}_h$, and φ_h belongs to an auxiliary space Φ_h satisfying

$$\text{grad } \Phi_h \subset \mathfrak{X}_h .$$

Note:

- ☹️ Since \mathfrak{X}_h consists of globally continuous functions, Φ_h must consist of **globally C^1 functions**.
- 😊 The space Φ_h **is not used** in the computations, but only in the estimation of the approximation error.

B-S decomposition suitable for the h version

Suitable hypotheses on the weight, smooth right hand side (or EV problem), 2D, ...

Theorem: The solution can be decomposed as $u = w + \text{grad } \varphi$,

with

$$w \in H^{1+\tau}(\Omega)$$

and

$$\varphi \in \bigcap_{m=0}^{\infty} K_{\beta}^m$$

Here (2D, one reentrant corner of opening ω) $H^{1+\tau}$ is the regularity of the Neumann problem for the Laplace operator in Ω , i.e. $\tau < \pi/\omega$, and β is determined by the regularity of the Dirichlet problem, $\beta > -1 - \pi/\omega$.

The weighted Sobolev spaces K_{β}^m are defined by the seminorms

$$|\varphi|_{K_{\beta}^m}^2 = \sum_{|\alpha|=m} \|r^{\beta+|\alpha|} \partial^{\alpha} \varphi\|_{L^2}$$

Result: Energy norm estimate of order $O(h^{\tau})$ for any mesh that allows C^1 elements.

B-S decomposition suitable for the hp version

At present: Ω has to be a polygon in \mathbb{R}^2 .

Weighted spaces of analytic functions, compare BABUŠKA-GUO:

$$A_\beta(\Omega) \subset \bigcap_{m=0}^{\infty} K_\beta^m(\Omega), \quad \exists C : \forall m : |\varphi|_{K_\beta^m} \leq C^{m+1} m!$$

One assumes that the right hand side is analytic (true for EVP), for example in $A_0(\Omega)^2$.

Theorem: For $\gamma \in (\gamma_\Omega, 1]$ there is a $\delta_\gamma > 0$ such that for all $0 < \delta < \delta_\gamma$, the solution u can be decomposed as $u = w + \text{grad } \varphi$,

with $w \in A_{-1-\delta}(\Omega)^2$

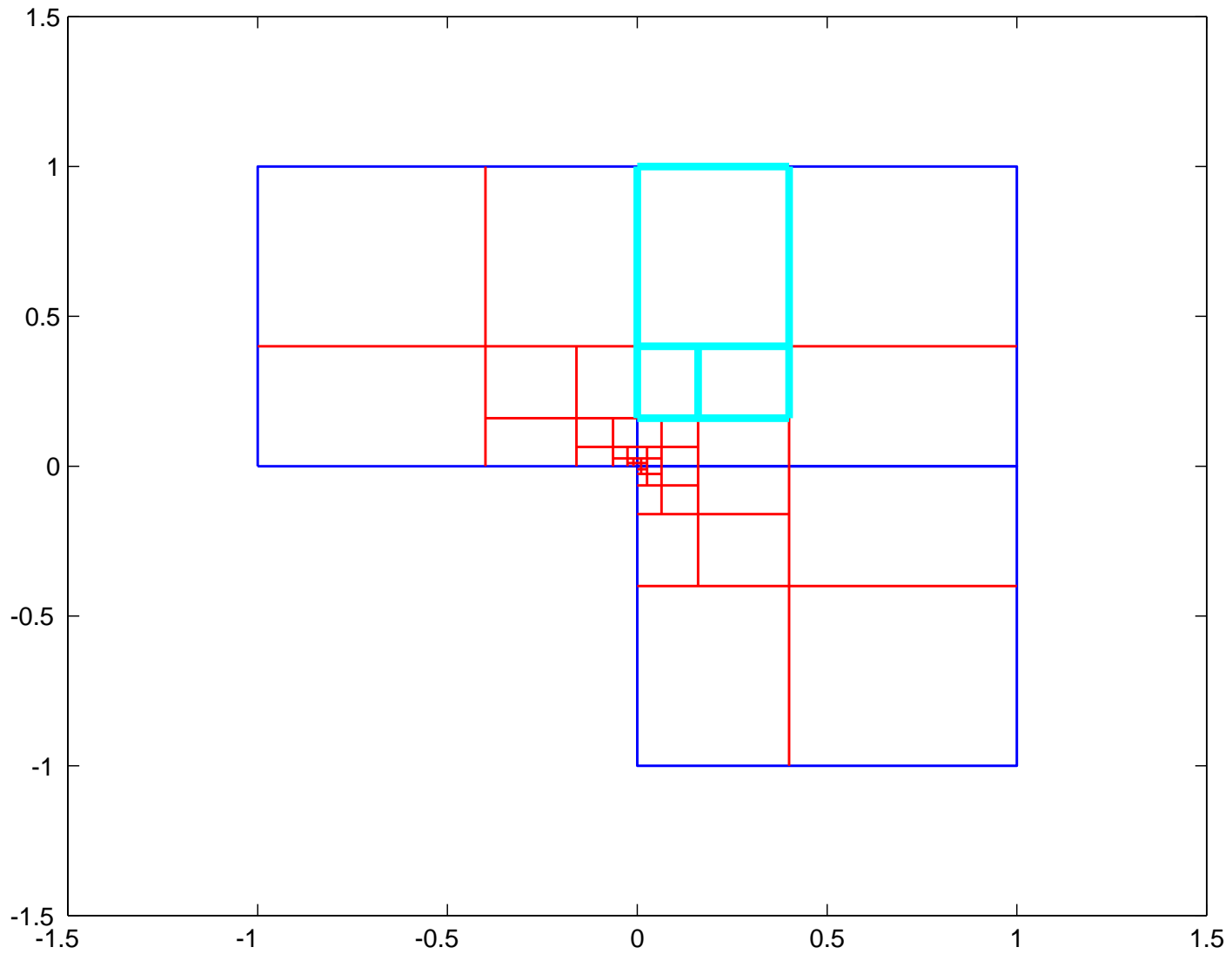
and $\varphi \in H_0^1 \cap A_{\gamma-1-\delta}(\Omega)$

Result: For suitably (geometrically) refined meshes, one has an energy norm error estimate of order $O(e^{-bp})$ for some $b > 0$.

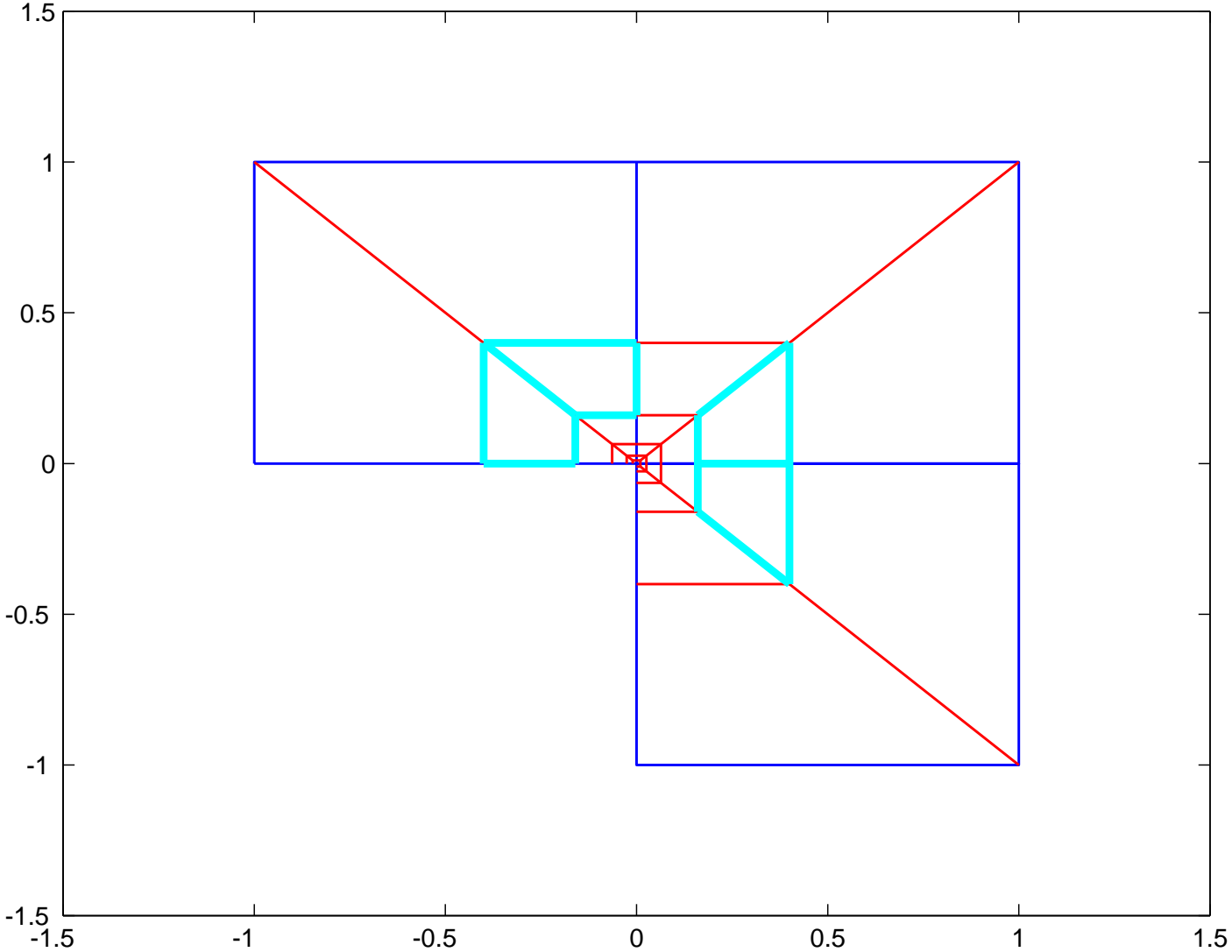
**For the analysis of the hp version,
3 types of exponentially refined meshes:**

In **CYAN**, the **patch** to consider for the construction of C^1 interpolants.

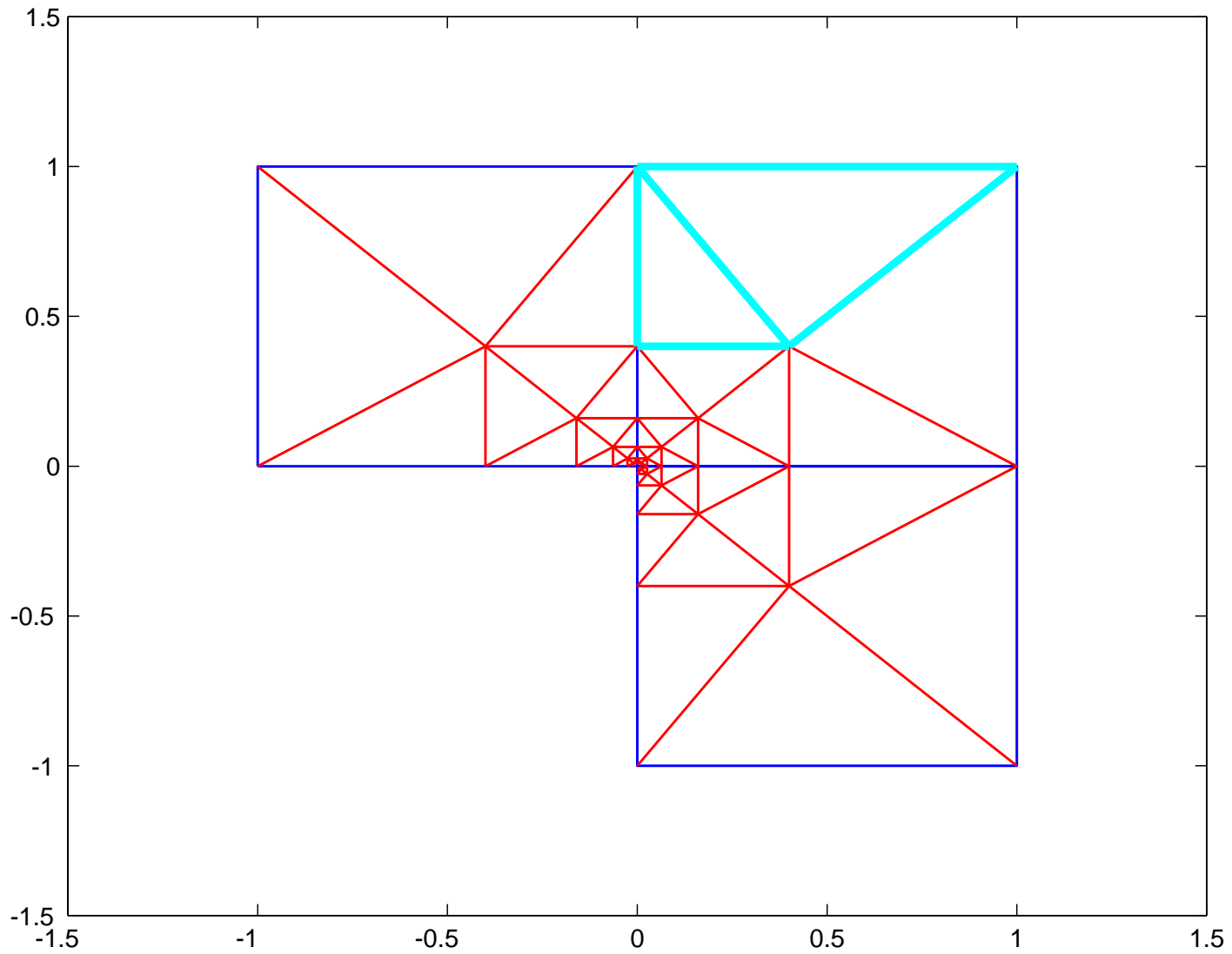
Rectangles with hanging nodes



Q^1 -quadrilaterals

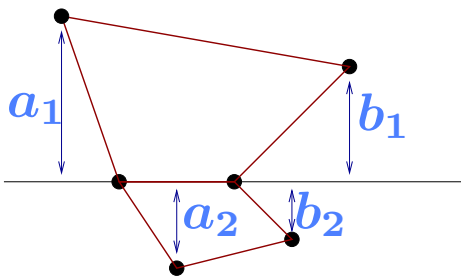


Triangles



Problems with Q^1 -quadrilaterals

- Polynomials on the reference square \widehat{K} are **not polynomials** on the physical element K , in general.
- The Jacobian $J \in \mathbb{P}^1(\widehat{K})$ is **not constant**, therefore the gradient (in physical space) does **not map** $Q^p(\widehat{K})$ into $Q^p(K)$.
- The (auxiliary) approximation FE space Φ_h for the potentials has to be chosen not as $Q^p(\widehat{K})$, but as $J^m \cdot Q^{p-m}(\widehat{K})$ (depends on K !), for some $m \geq 3$.
- There is a geometrical condition on the **patches** (the jacobians J on both sides have to be proportional on the interface) which is not always satisfied, **but satisfied in our case of the L and two axiparallel sides.**

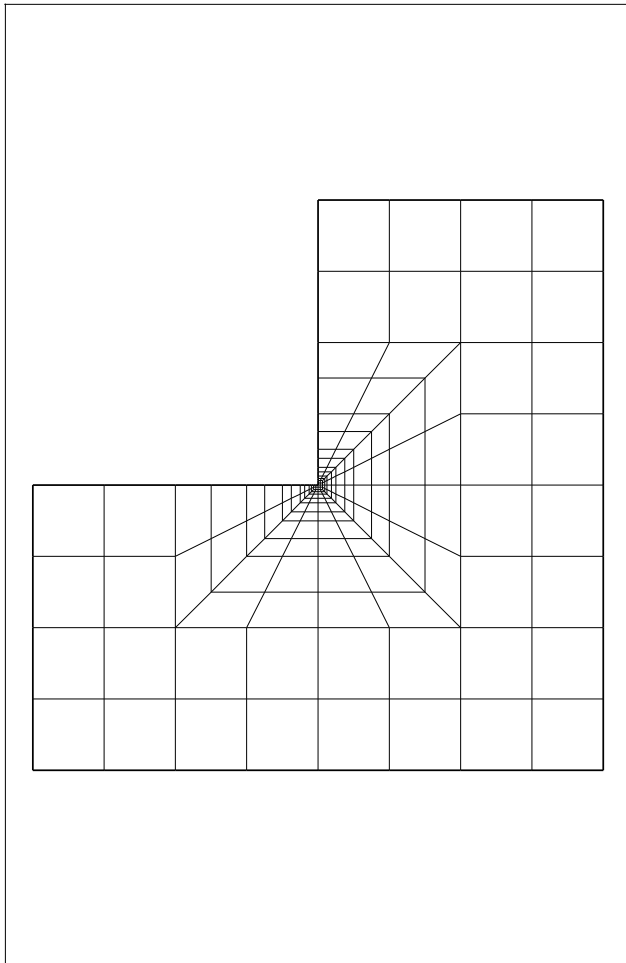


$$\frac{a_1}{b_1} = \frac{a_2}{b_2}$$

Computations in 2D

The straight L:

Ω is the *L*-shaped domain : $[0.5, 1] \times [0.5, 1] \setminus [0.75, 1] \times [0.75, 1]$.



Computation of the first 15 eigenvalues $\Lambda[s]$ for

$$s = [2 : 100],$$

$$\alpha = 0, 1, 2,$$

$$q = 1, 2, 3, 4$$

The computed eigenvalues are sorted depending on whether

$$\frac{\|\operatorname{curl} u\|^2}{s \|\mathcal{r}^{\alpha/2} \operatorname{div} u\|^2}$$

is $\geq \rho$ or $\leq \rho^{-1}$ with a fixed $\rho \geq 1$.

Legend

For the next 8 figures.

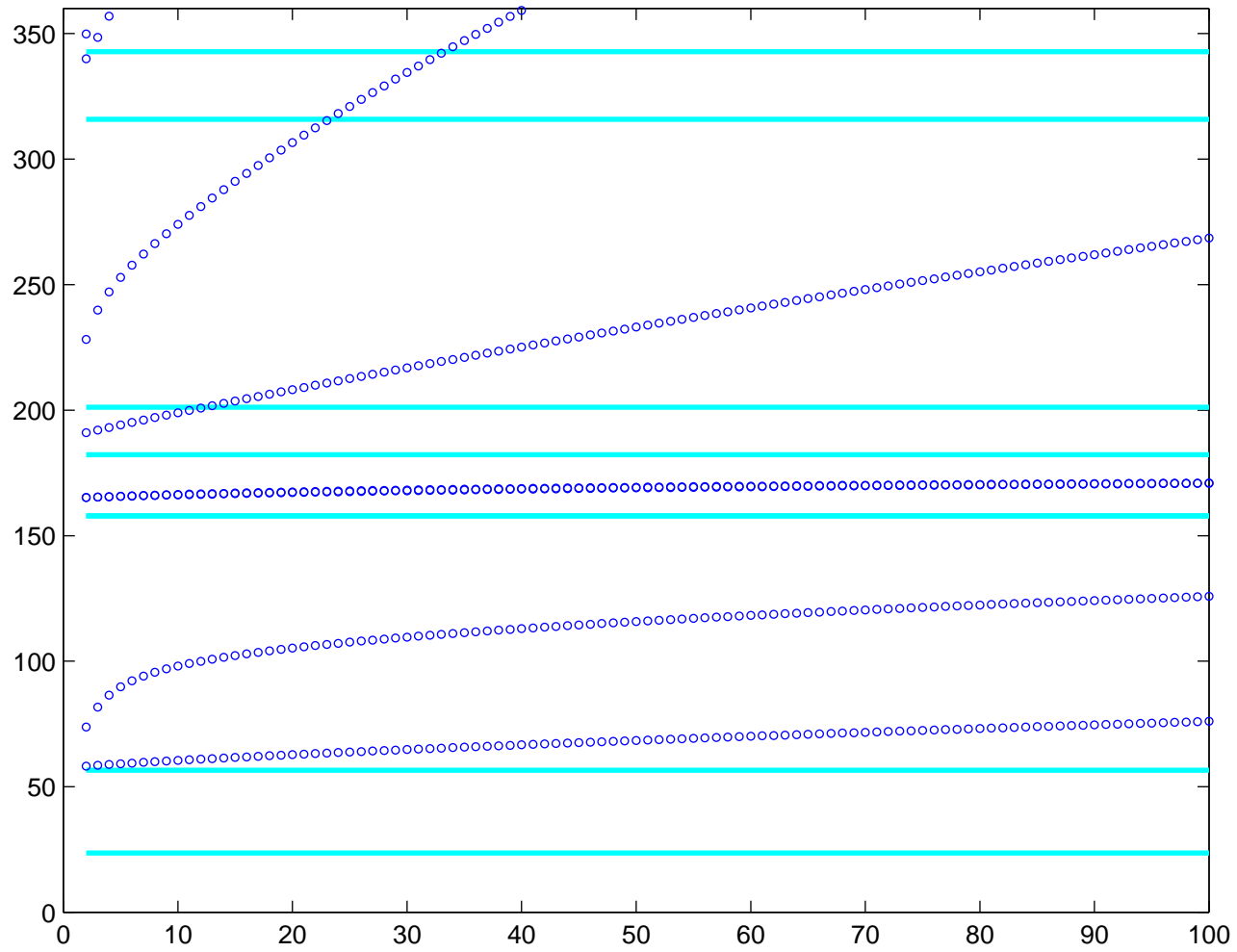
In *Cyan*, the Laplace-Neumann eigenvalues, which coincide for 2D domains with Maxwell eigenvalues.

In *Blue*, the circles represent the computed $\Lambda[s]$ with curl-dominant eigenvectors.

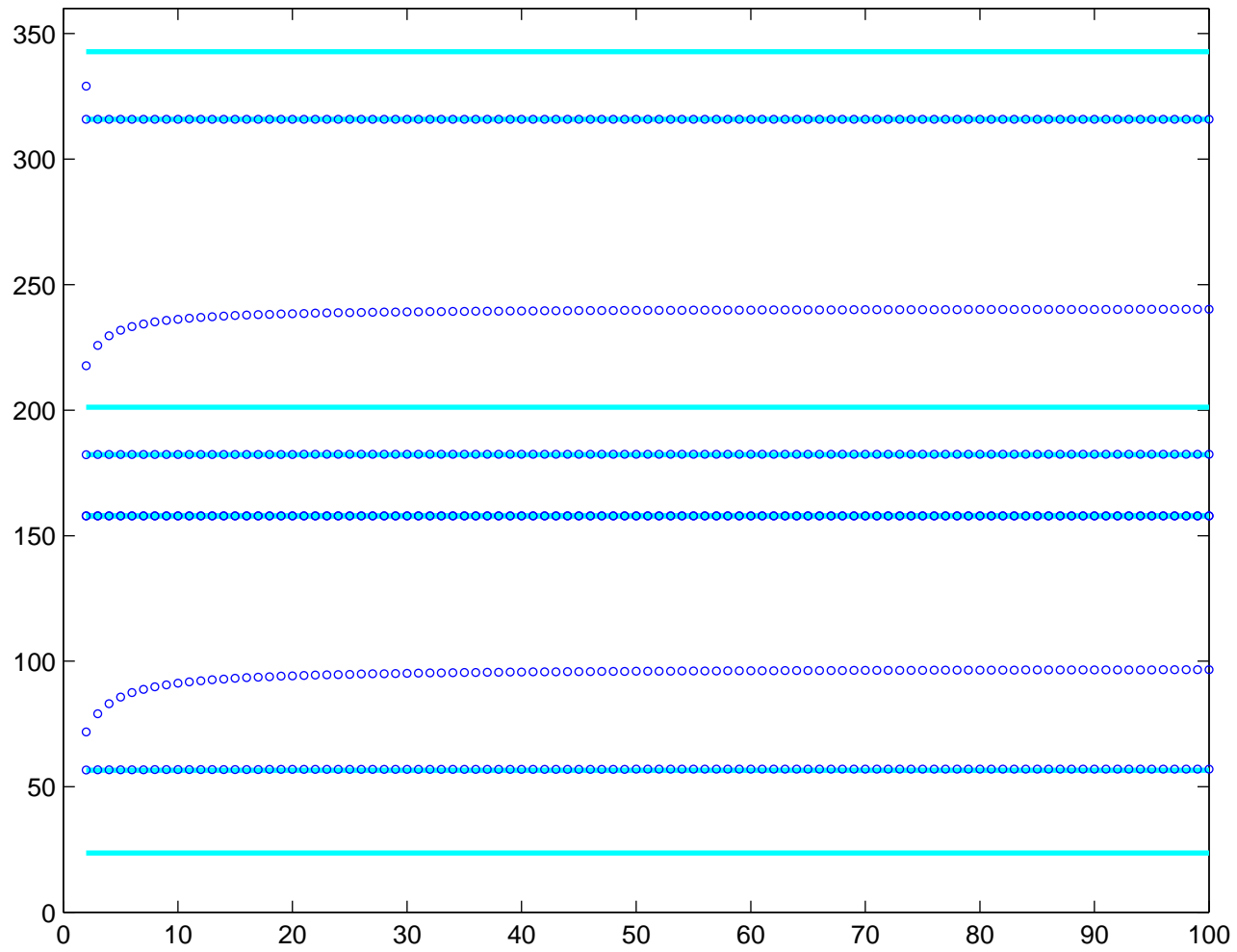
In *Red*, the lines join the computed $\Lambda[s]$ with div-dominant eigenvectors.

Abscissa : s / Ordinate : $\Lambda[s]$.

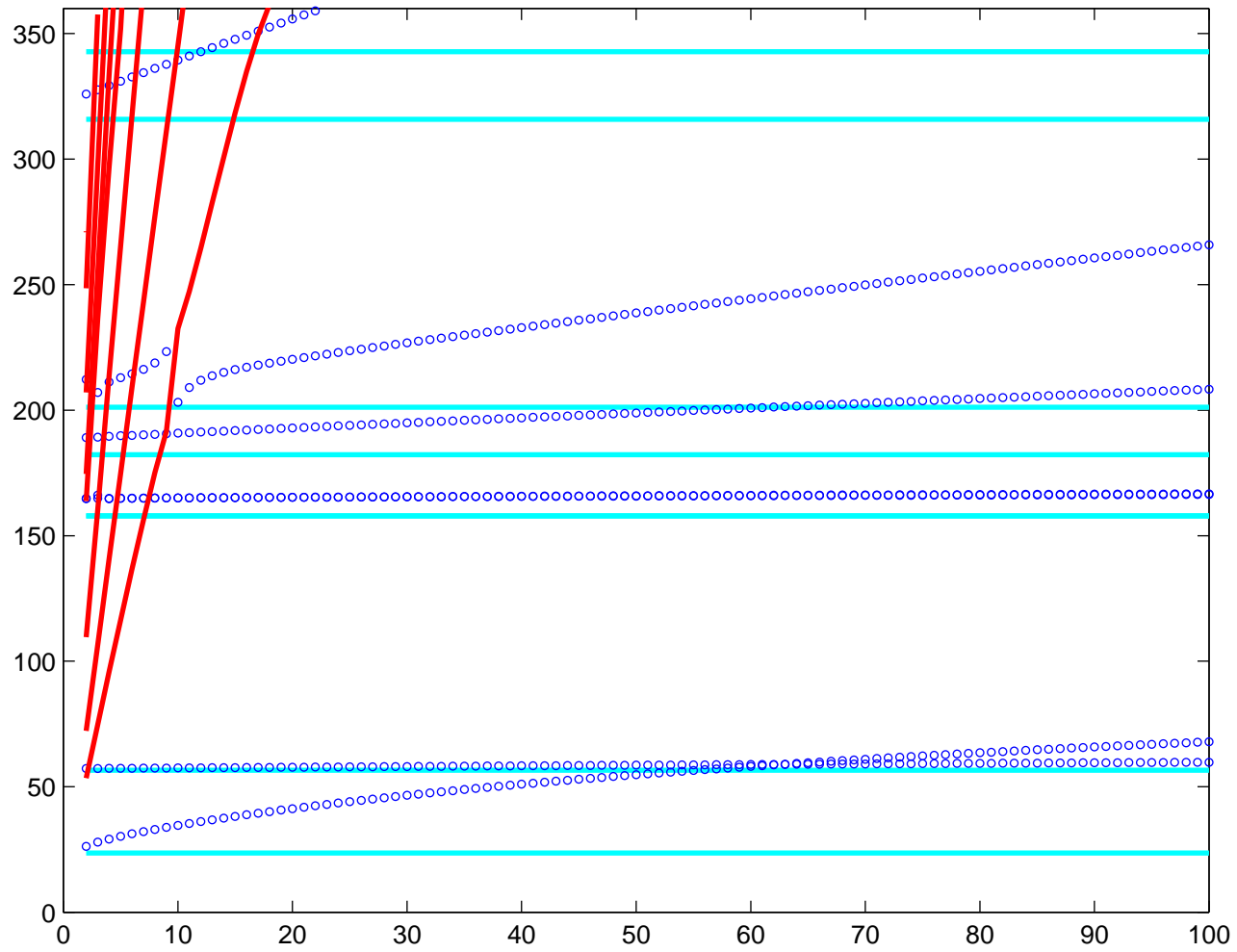
$$q = 1, \alpha = 0$$



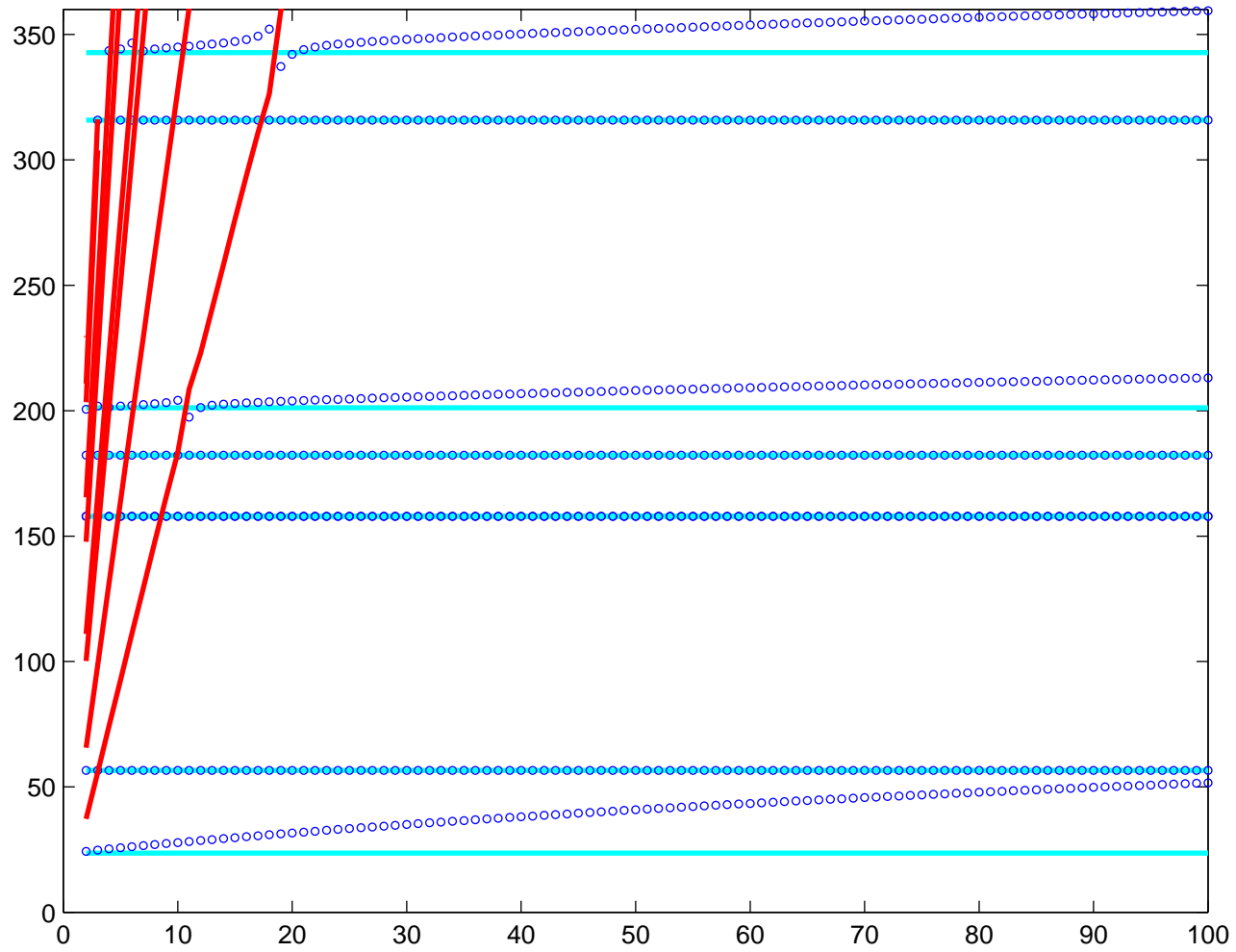
$$q = 4, \alpha = 0$$



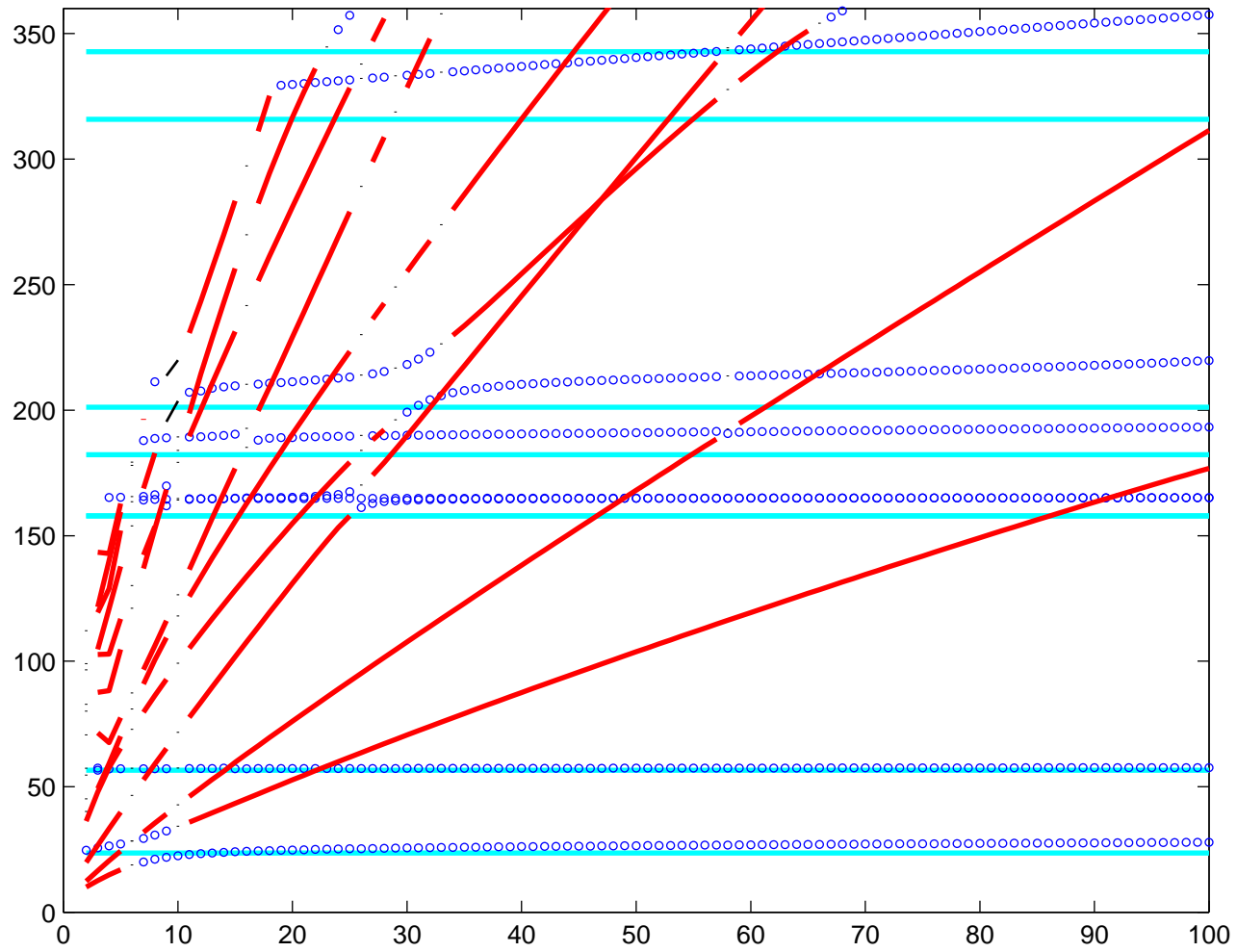
$q = 1, \alpha = 1$



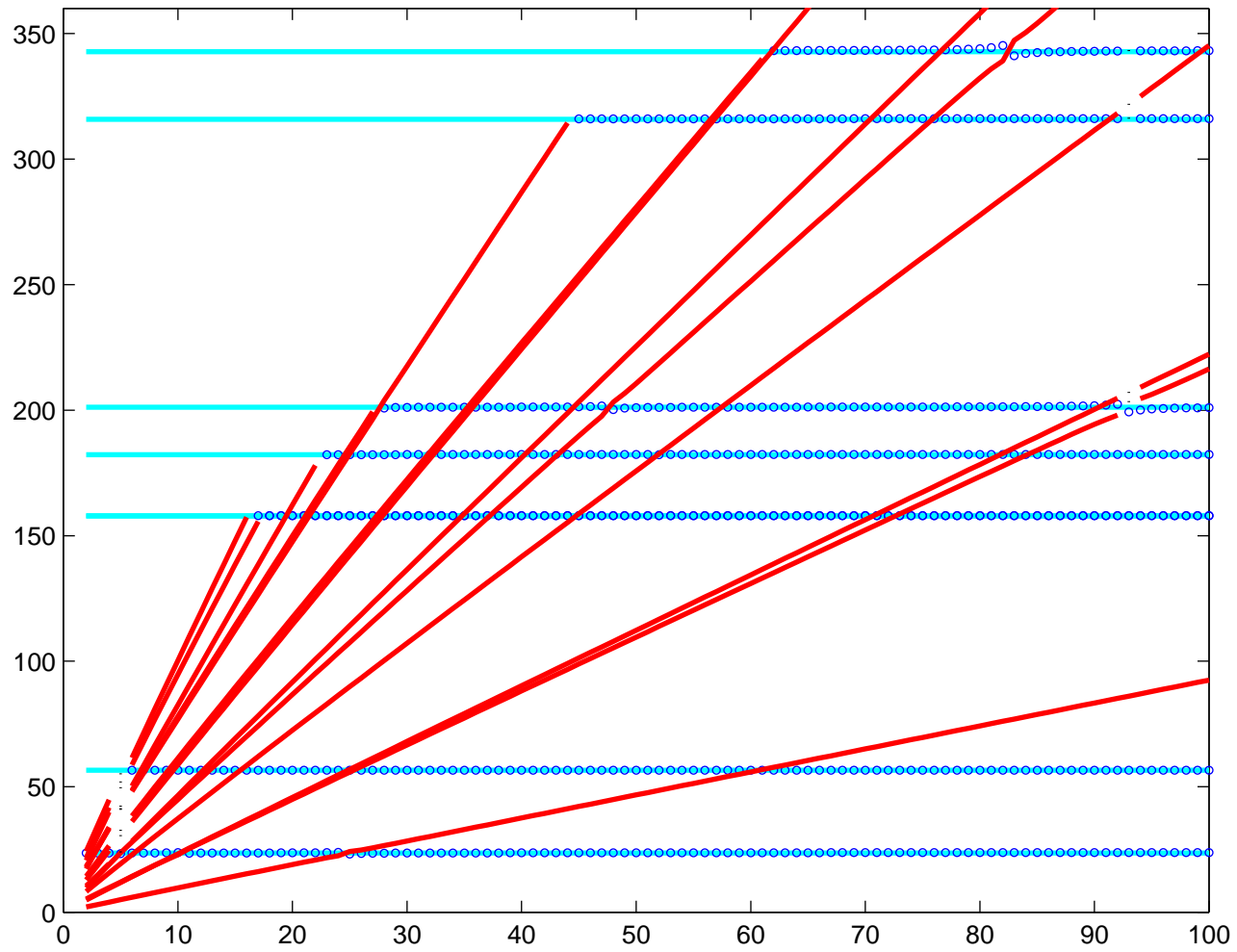
$$q = 4, \alpha = 1$$



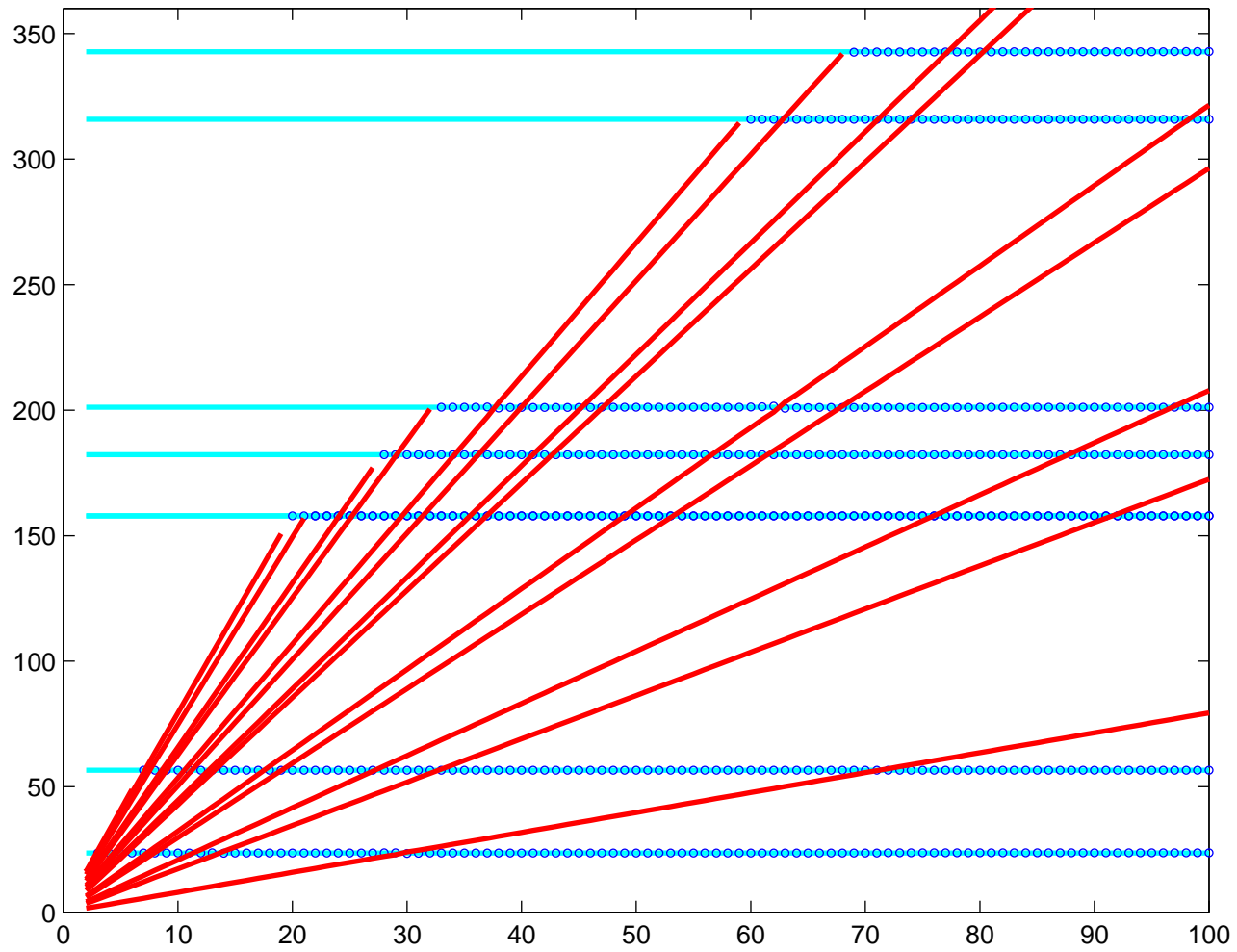
$q = 1, \alpha = 2$



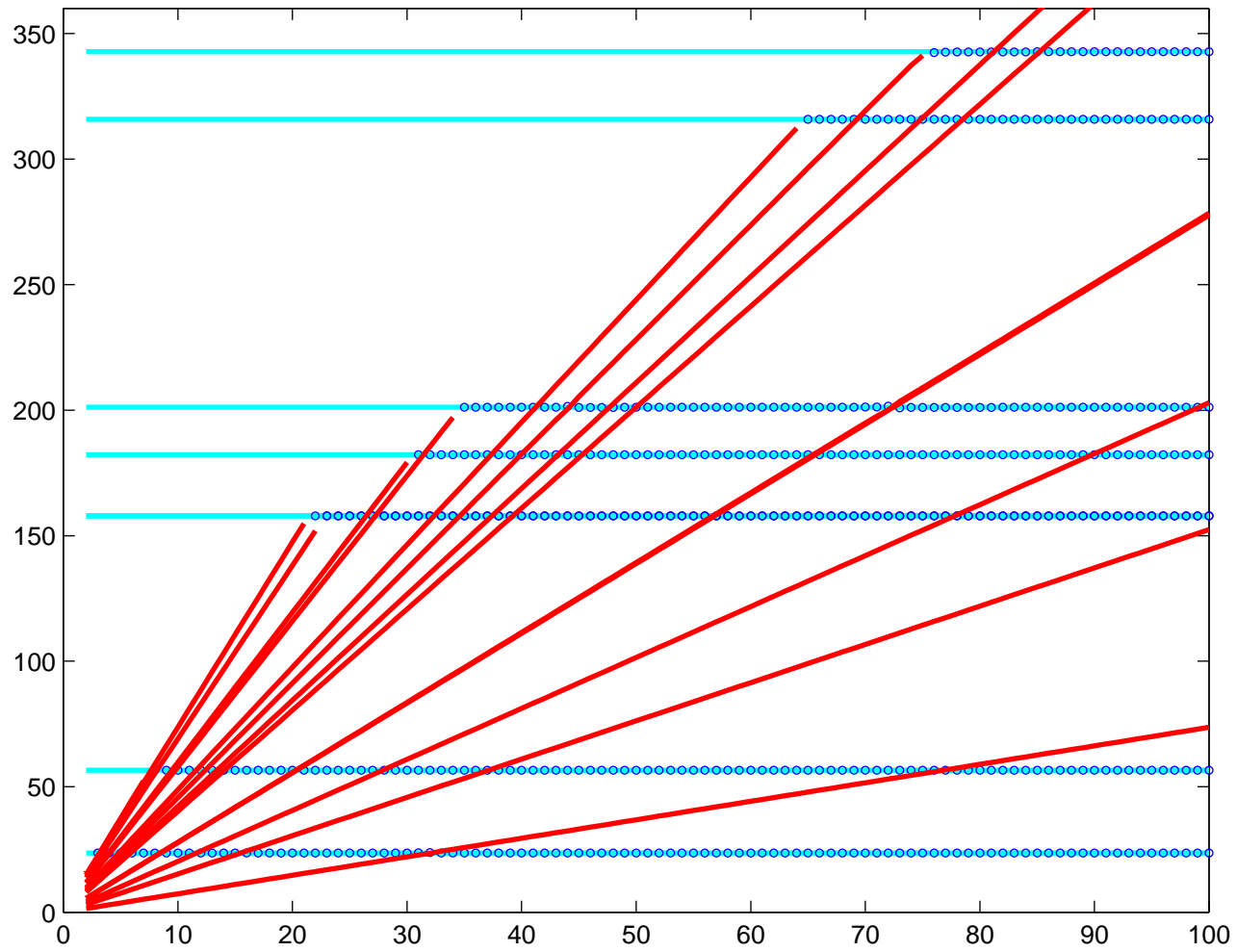
$q = 2, \alpha = 2$



$$q = 3, \alpha = 2$$

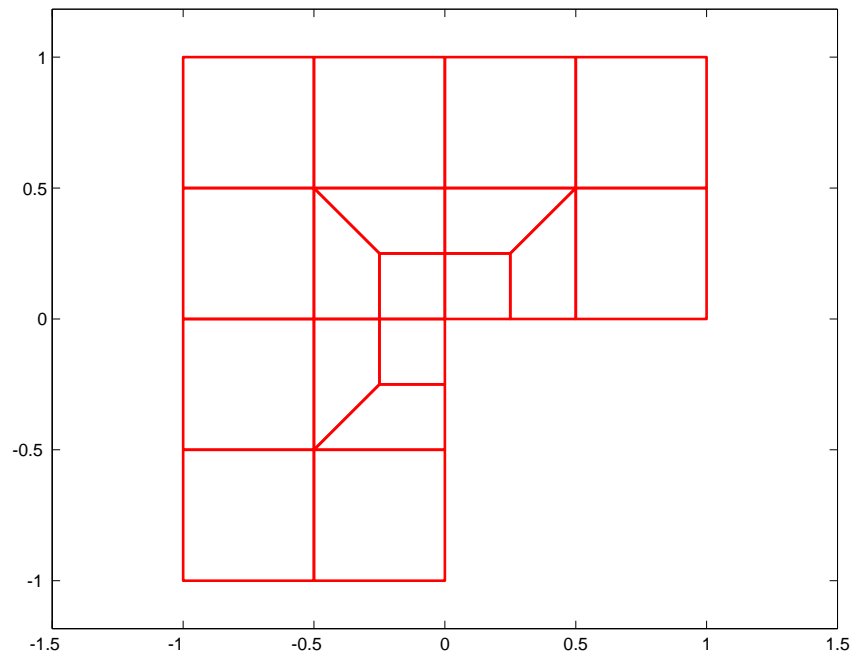


$$q = 4, \alpha = 2$$

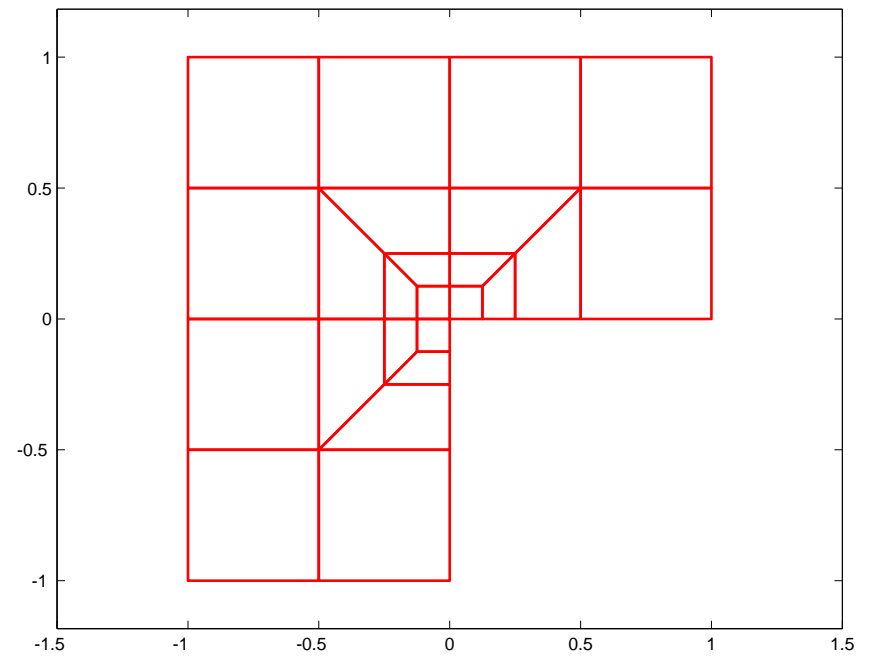


Geometrical mesh refinement, on straight L-shape domain (sL)

Ratio 2.



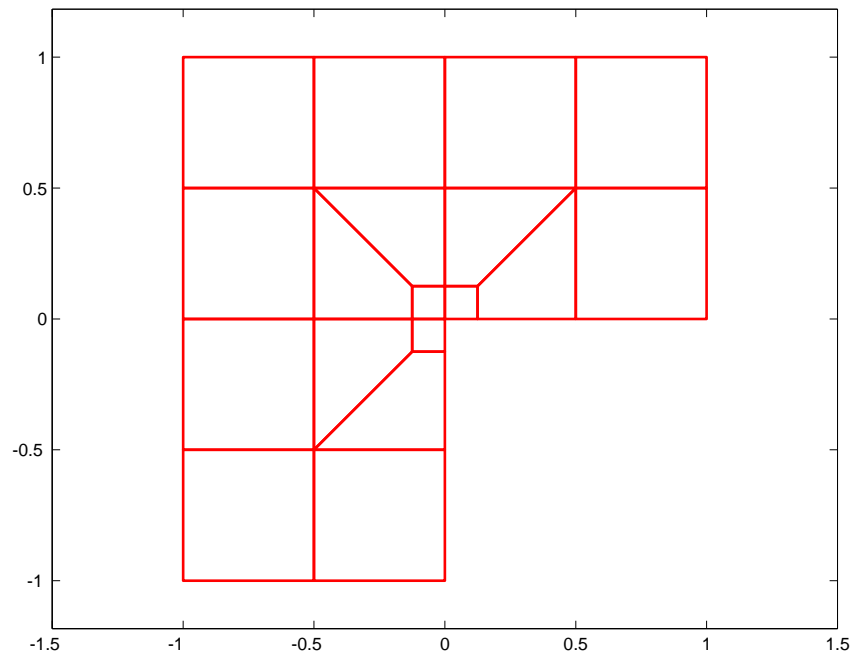
3 layers.



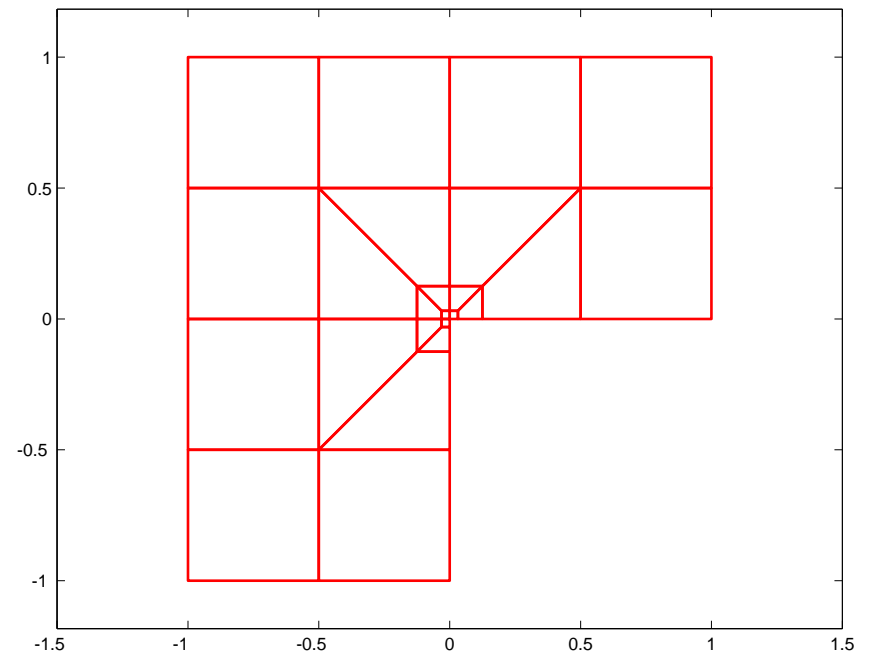
4 layers.

Geometrical mesh refinement, on straight L-shape domain (sL)

Ratio 4.



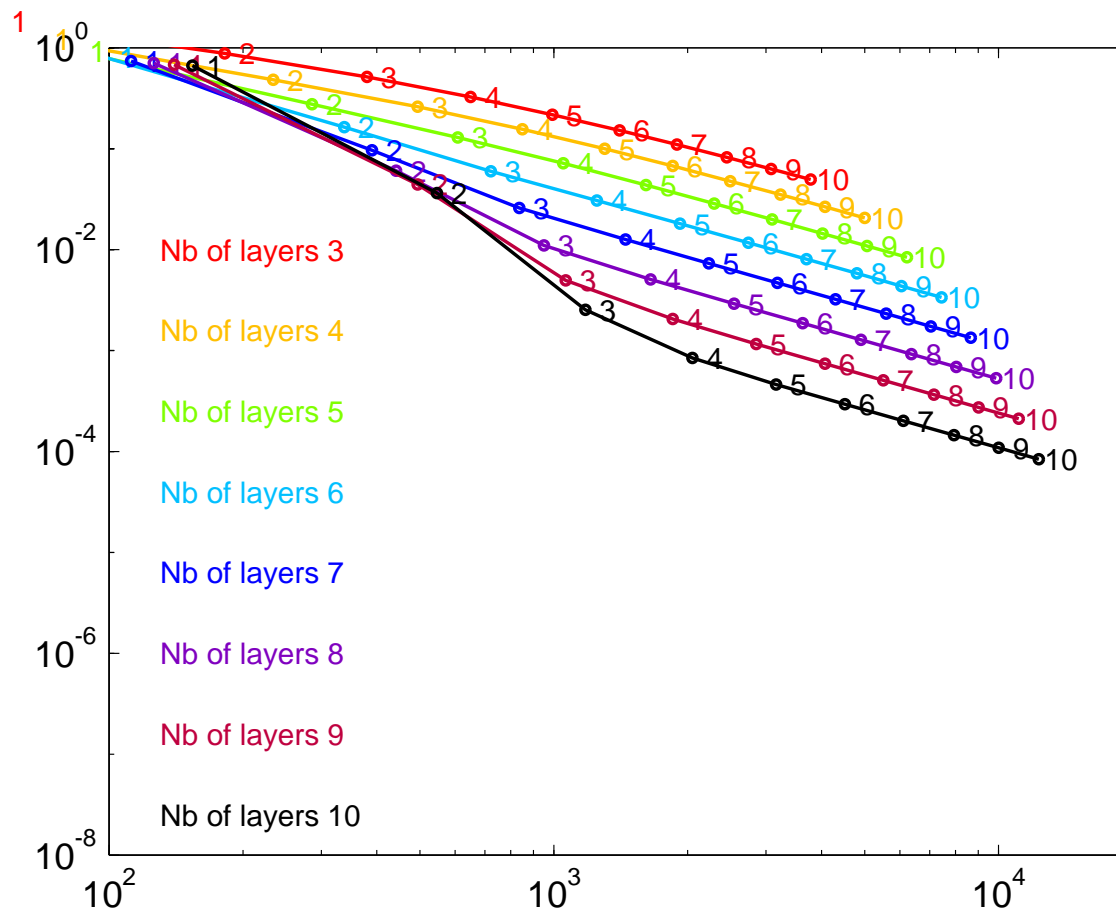
3 layers.



4 layers.

First Maxwell ev. on L-domain, with $\alpha = 2$ and ref. ratio 2

On domain (sL) with number of layers $3 \leq m \leq 10$ & funct. interp. $1 \leq p \leq 10$.



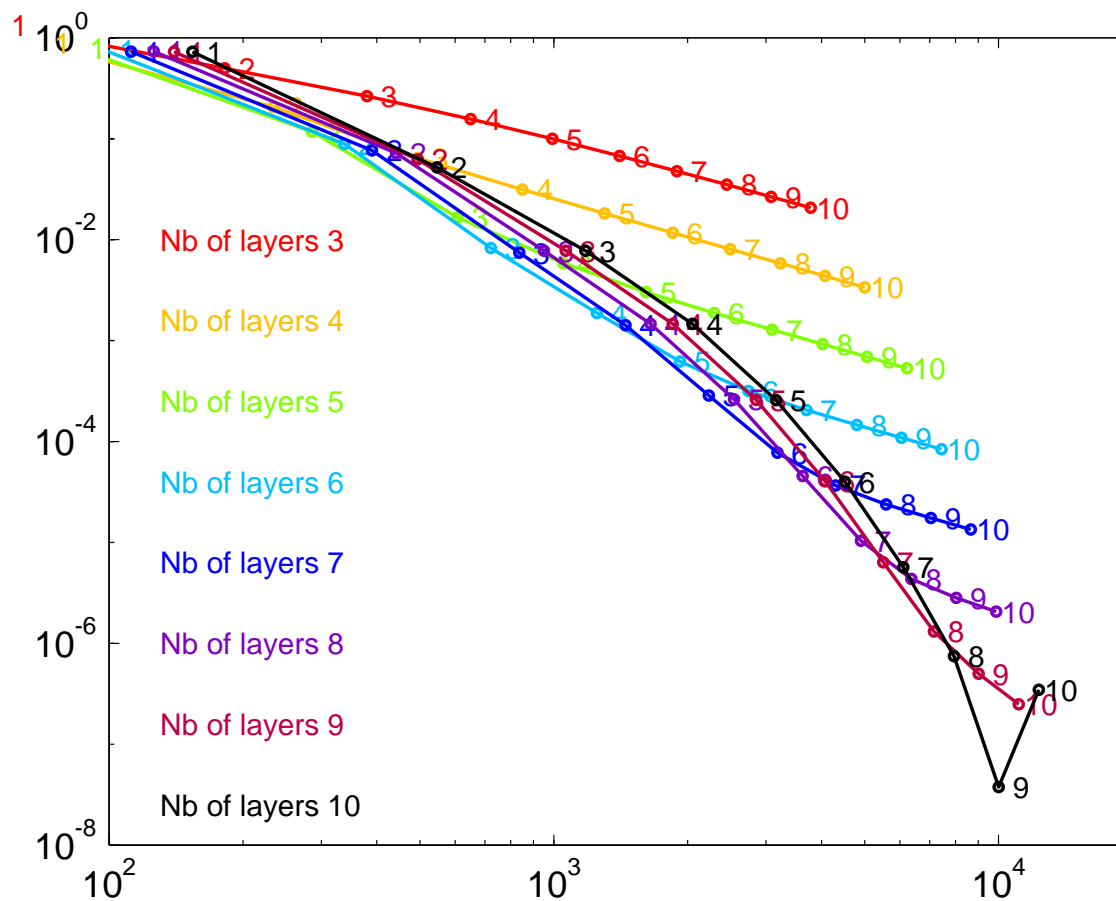
Relative error
versus the number of
DOF.

Computed with MÉLINA

FEM library
developped by
D. MARTIN
(Rennes, ENSTA).

First Maxwell ev. on L-domain, with $\alpha = 2$ and ref. ratio 4

On domain (sL) with number of layers $3 \leq m \leq 10$ & funct. interp. $1 \leq p \leq 10$.



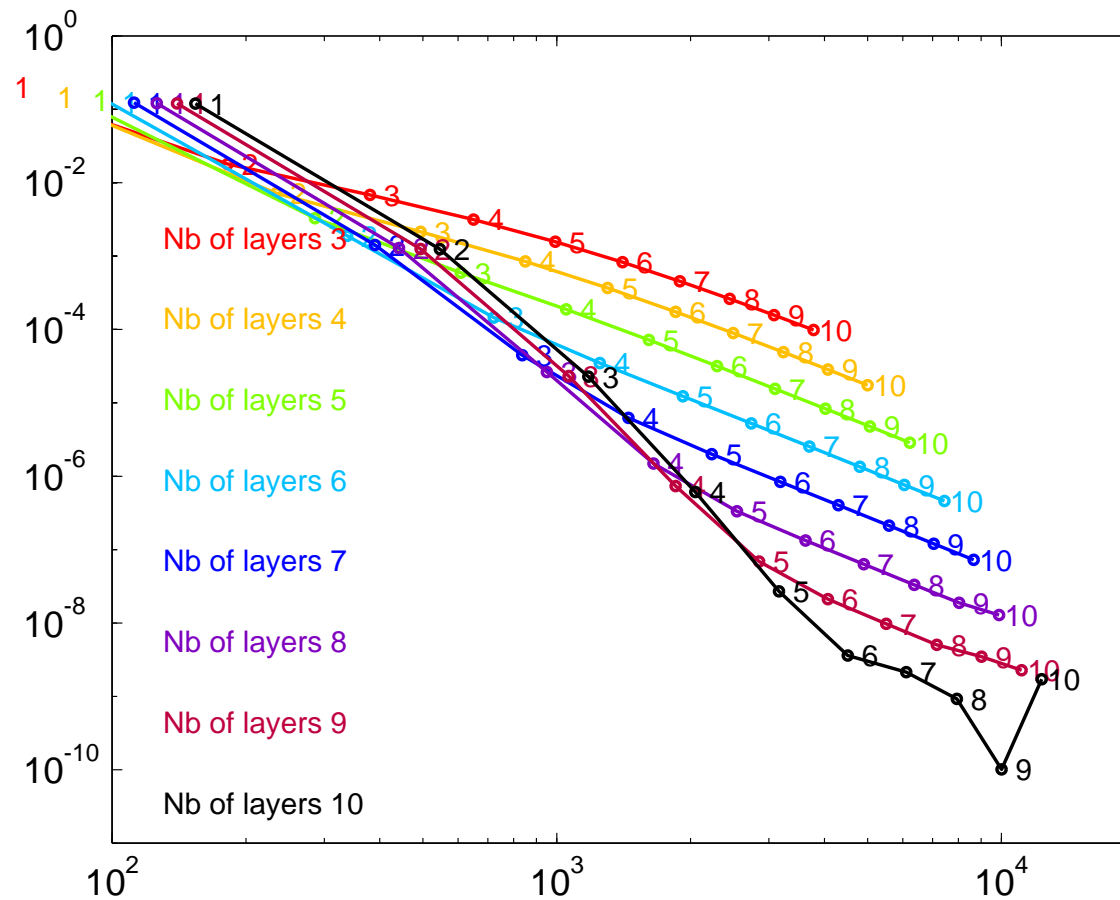
Relative error
versus the number of
DOF.

Computed with MÉLINA

FEM library
developped by
D. MARTIN
(Rennes, ENSTA).

Second Maxwell ev. on L-domain, with $\alpha = 2$ and ref. ratio 2

On domain (sL) with number of layers $3 \leq m \leq 10$ & funct. interp. $1 \leq p \leq 10$.



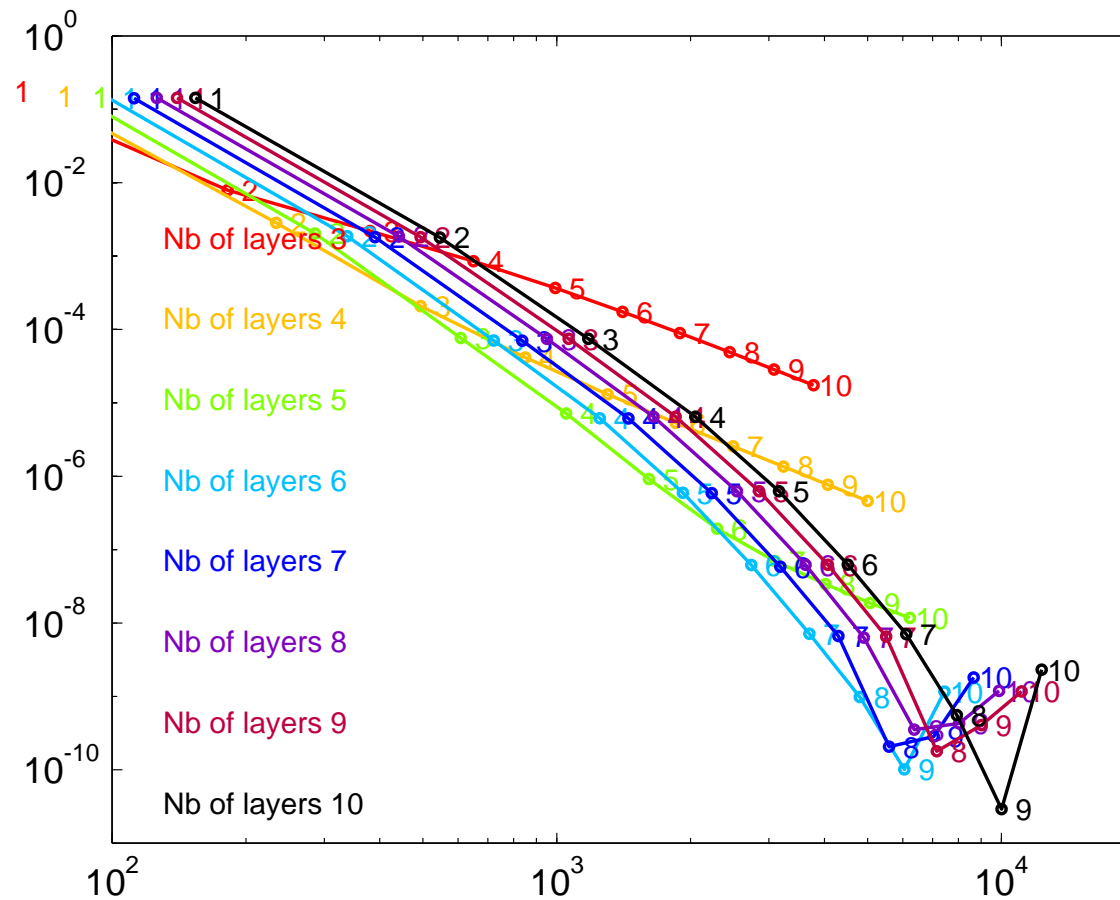
Relative error
versus the number of
DOF.

Computed with MÉLINA

FEM library
developped by
D. MARTIN
(Rennes, ENSTA).

Second Maxwell ev. on L-domain, with $\alpha = 2$ and ref. ratio 4

On domain (sL) with number of layers $3 \leq m \leq 10$ & funct. interp. $1 \leq p \leq 10$.

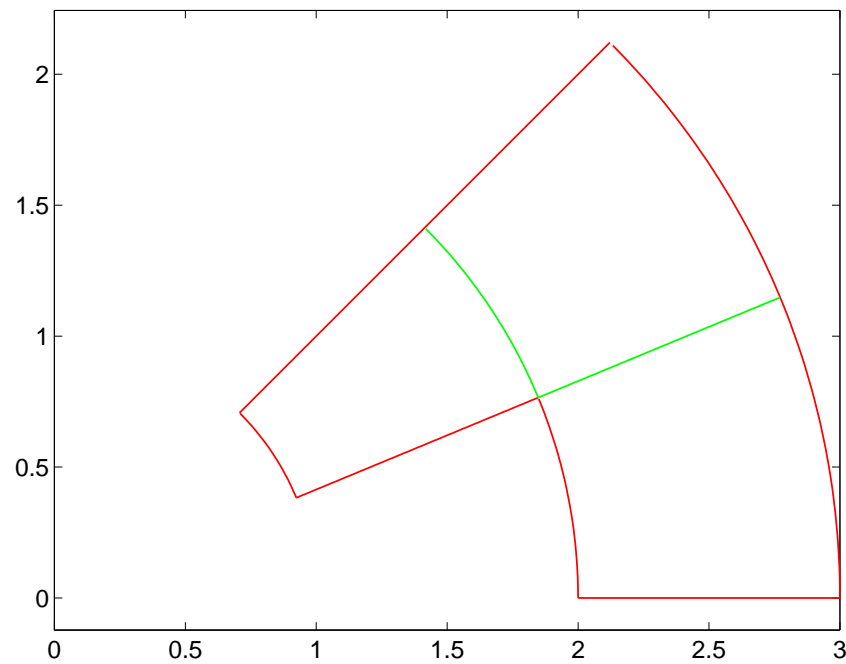


Relative error
versus the number of
DOF.

Computed with MÉLINA

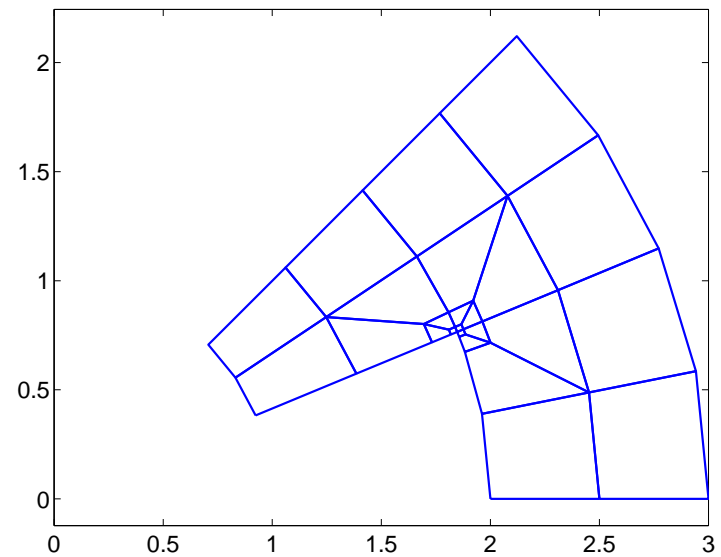
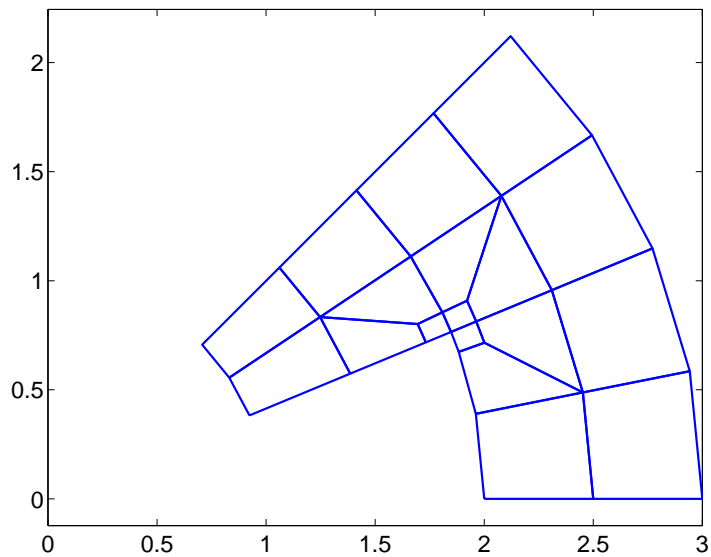
FEM library
developped by
D. MARTIN
(Rennes, ENSTA).

Curved L-shaped domain



**The curved L-shaped domain (cL)
with a $2\pi/3$ corner.**

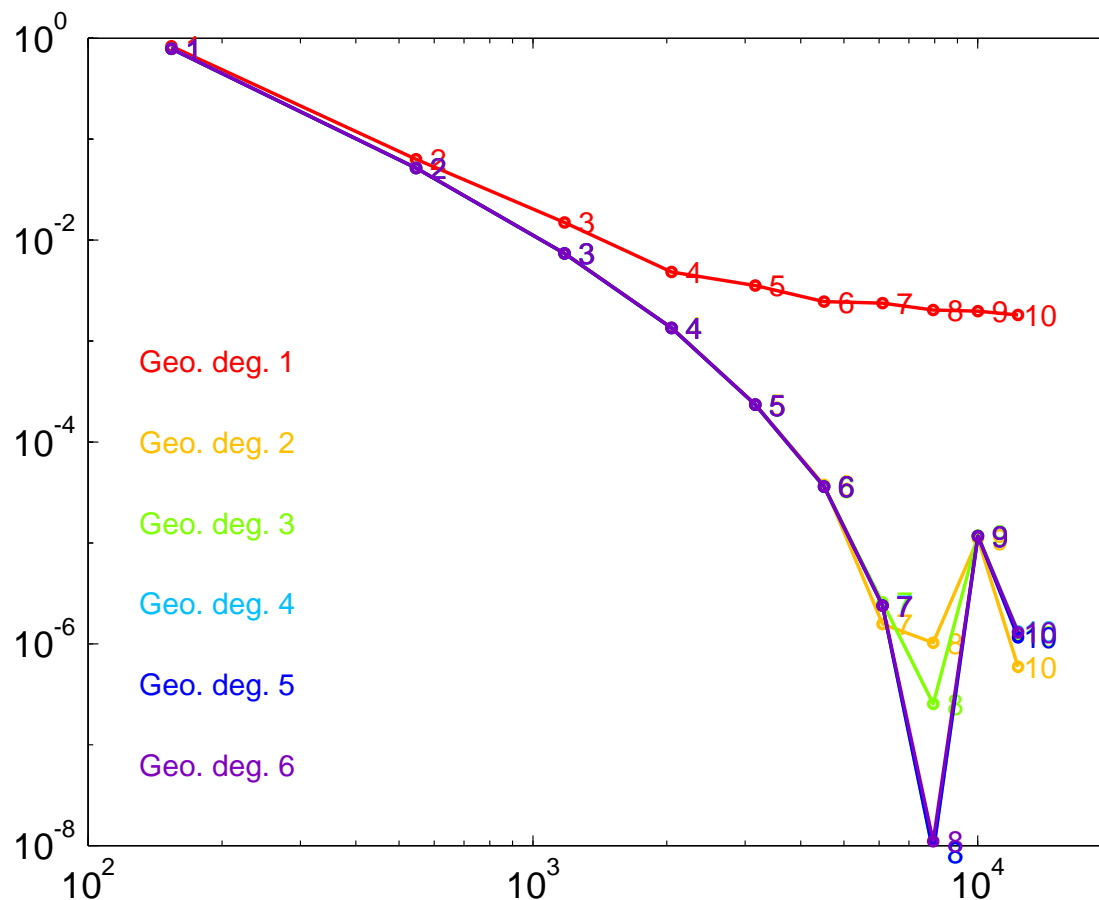
Meshes on the approximate curved L-domain



$$\Omega_{q,m}, q = 1, m = 3, 4$$

First Maxwell ev. on curved L, with weight & refinement

On domain (cL) with **ratio 4**, number of layers $m = 10$, and $\alpha = 2$.



Geom. interp.

$$1 \leq n \leq 6$$

& Funct. interp.

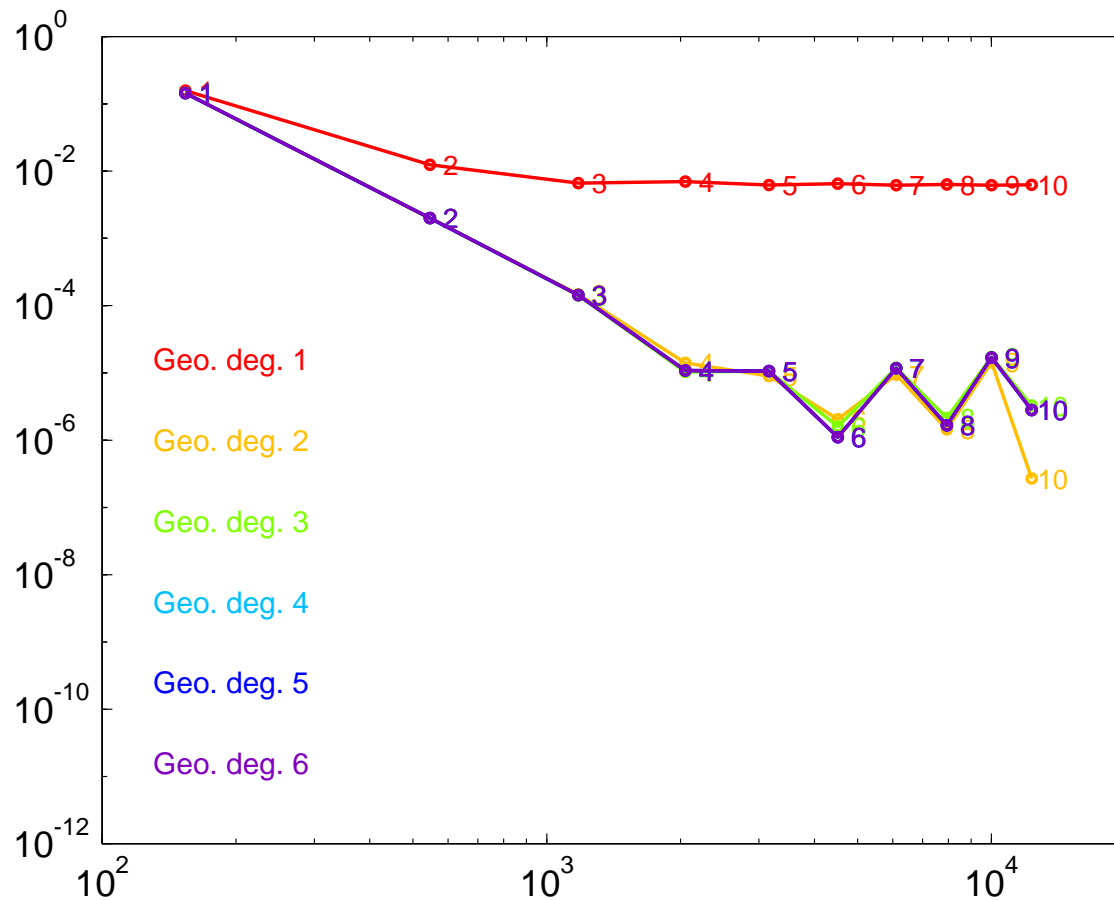
$$1 \leq p \leq 10.$$

Relative error
versus the number of
DOF.

Computed with MÉLINA.

Second Maxwell ev. on curved L, with weight & refinement

On domain (cL) with **ratio 4**, number of layers $m = 10$ and $\alpha = 2$.



Geom. interp.

$$1 \leq n \leq 6$$

& Funct. interp.

$$1 \leq p \leq 10.$$

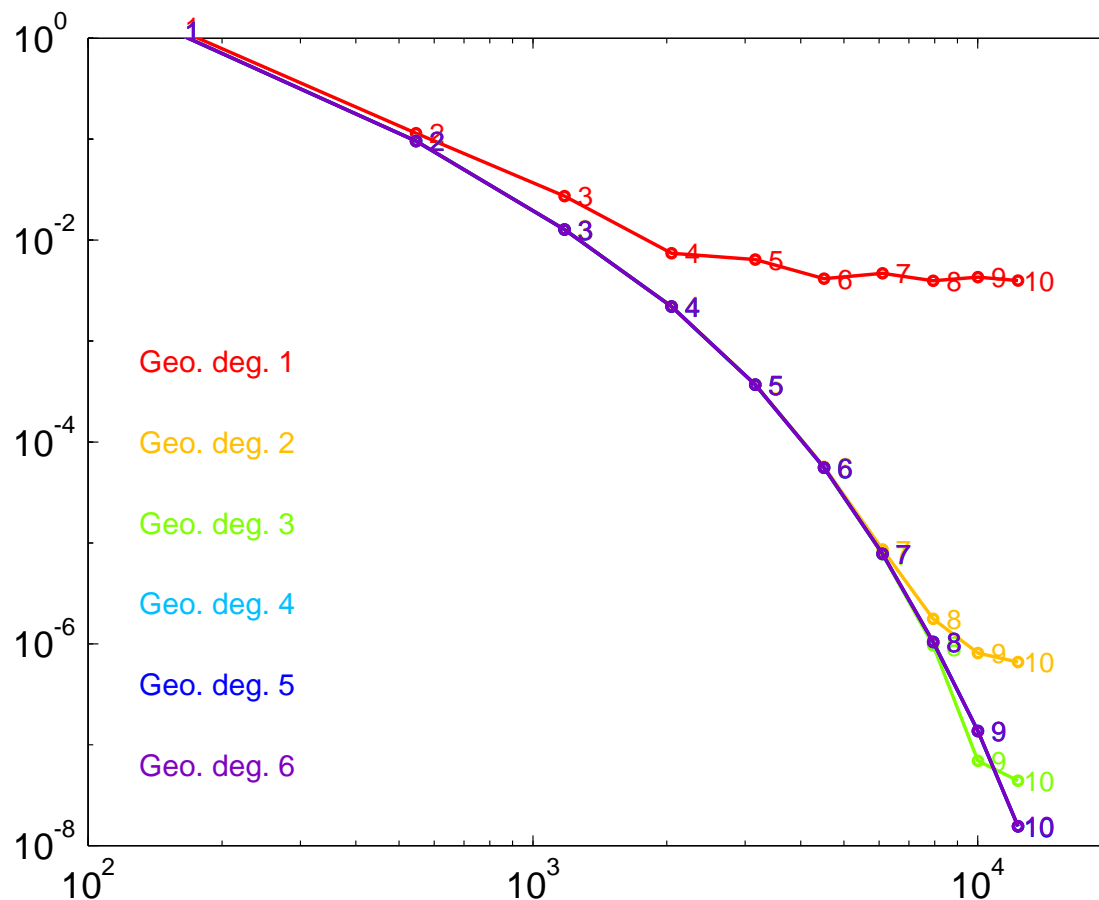
Relative error
versus the number of
DOF.

Computed with MÉLINA.

Something weird going
on here...

First Maxwell ev. on curved L, with weight & refinement

On domain (cL) with **ratio 4**, number of layers $m = 10$, and $\alpha = 2$.



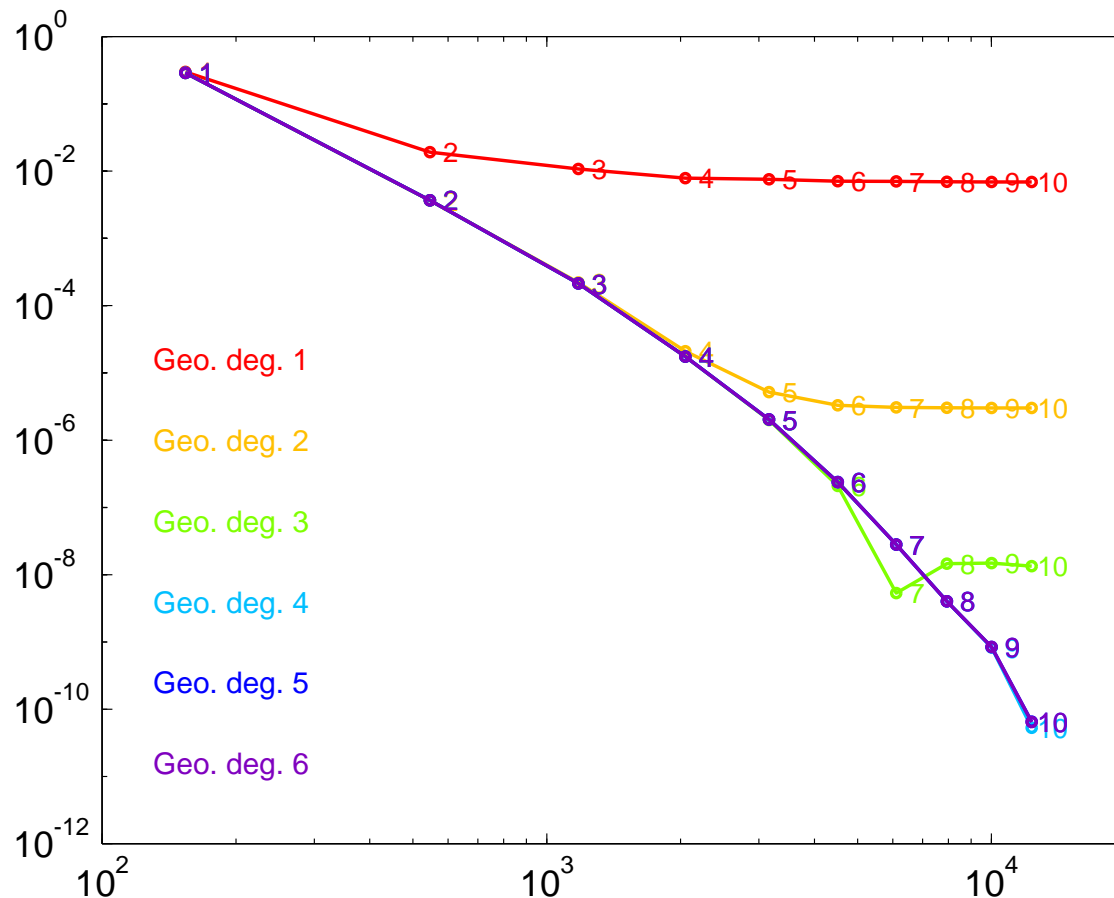
Nodes =
Gauss-Lobatto points.

Geom. interp.
 $1 \leq n \leq 6$
& Funct. interp.
 $1 \leq p \leq 10$.

Relative error
versus the # of DOF.

Second Maxwell ev. on curved L, with weight & refinement

On domain (cL) with **ratio 4**, number of layers $m = 10$ and $\alpha = 2$.



Nodes =
Gauss-Lobatto points.

Geom. interp.

$$1 \leq n \leq 6$$

& Funct. interp.

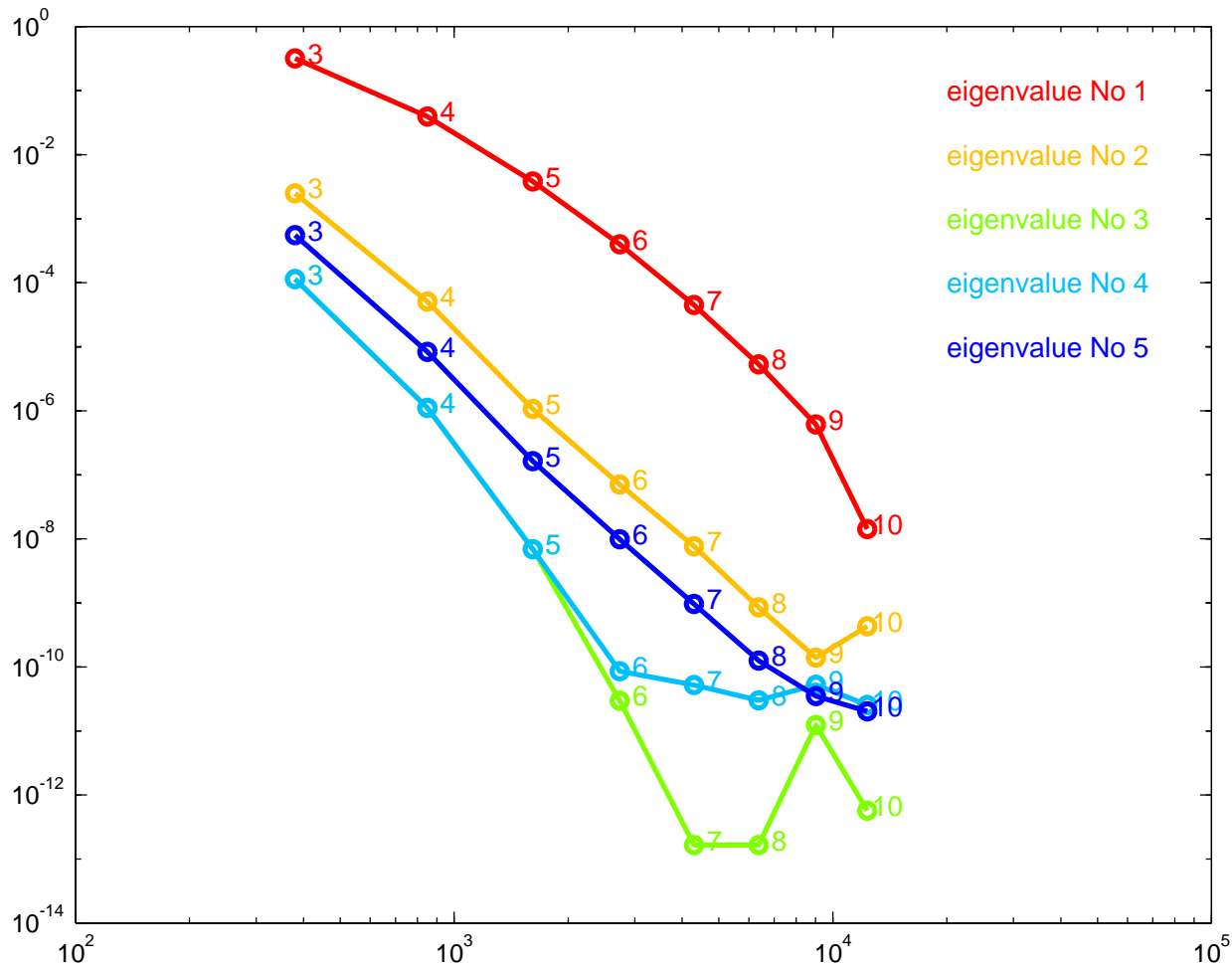
$$1 \leq p \leq 10.$$

Relative error
versus the # of DOF.

...this is much better!

Exponential convergence 1

Domain (sL) with ratio 4, $\alpha = 2$, 5 lowest eigenvalues.



h - p version:

$$3 \leq p = \#layers \leq 10$$

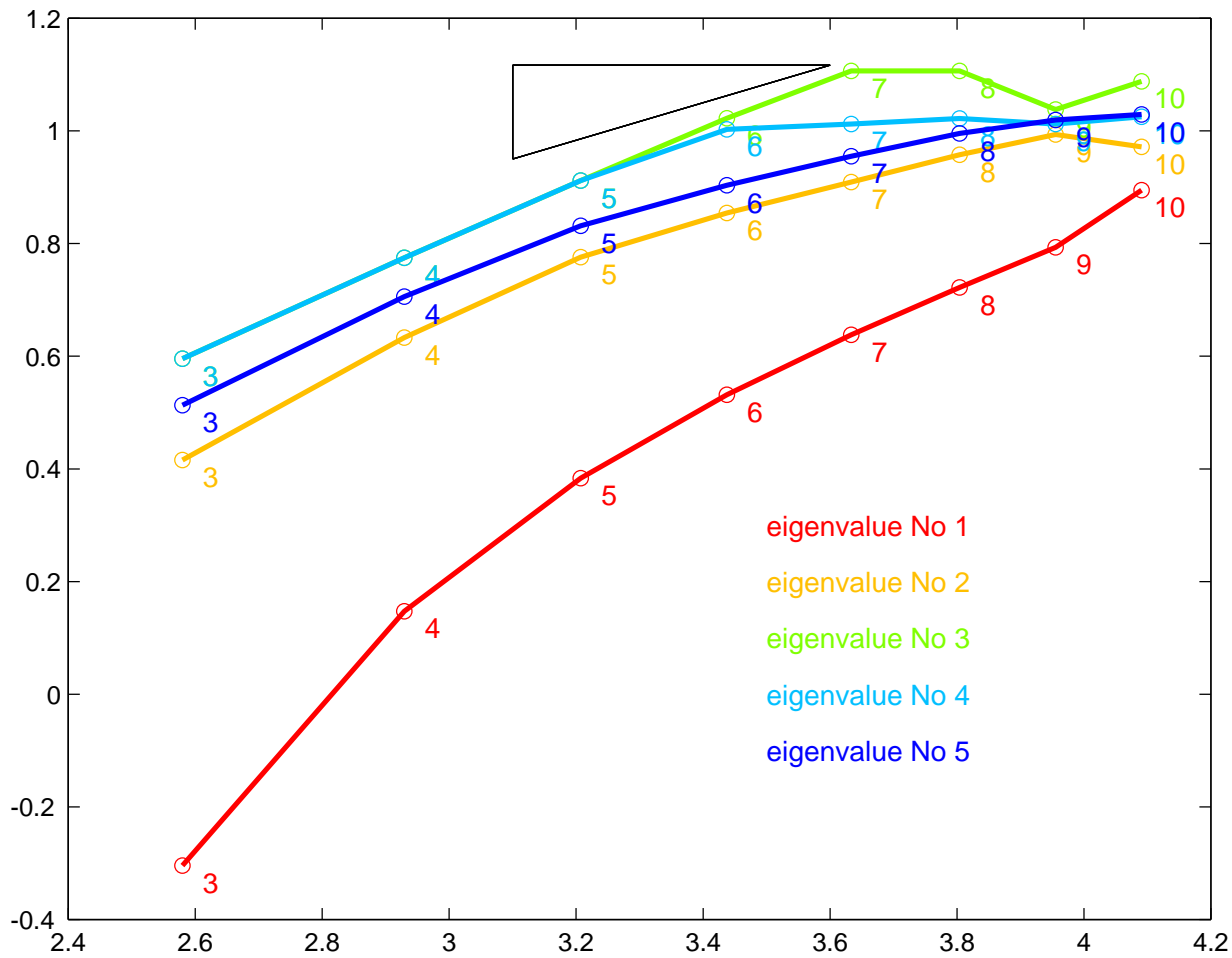
Relative error

VS

#DOF

Exponential convergence 2

Domain (sL) with **ratio 4**, $\alpha = 2$, 5 lowest eigenvalues.



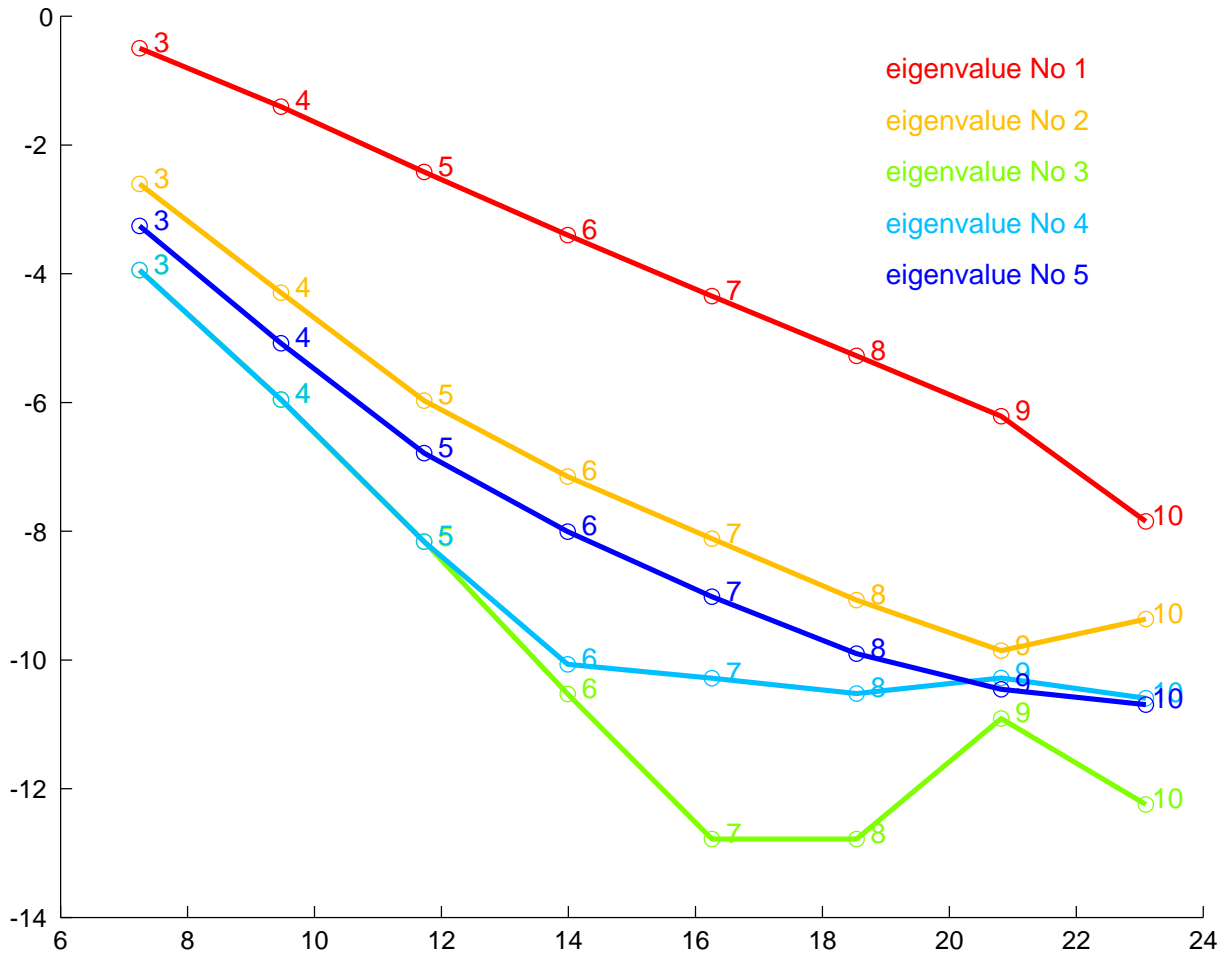
h - p version:

$$3 \leq p = \#layers \leq 10$$

log(-log(error))
VS
log(#DOF)

Exponential convergence 3

Domain (sL) with **ratio 4**, $\alpha = 2$, 5 lowest eigenvalues.



h - p version:

$$3 \leq p = \#layers \leq 10$$

log(error)
vs
(#DOF)^{1/3}

**3D hp version:
Computations are working nicely,
Theory: not yet finished...**

In the following graphs, we show results for two 3D domains:

- **The “thick L” $L \times [0, 1]$, where $L = [-1, 1]^2 \setminus [-1, 0]^2$ is the 2D straight L-shaped domain.**
- **Fichera’s corner (7/8th cube) $[-1, 1]^3 \setminus [-1, 0]^3$**

The Thick L: Legend

The Maxwell eigenvalues of the thick L $L \times [0, 1]$ are known:

They are **sums of Dirichlet and Neumann eigenvalues** of the 2D domain L (which can easily be computed to high precision) and of the interval $[0, 1]$ (which are of the form $\pi^2 n^2$, $n \in \mathbb{N}$).

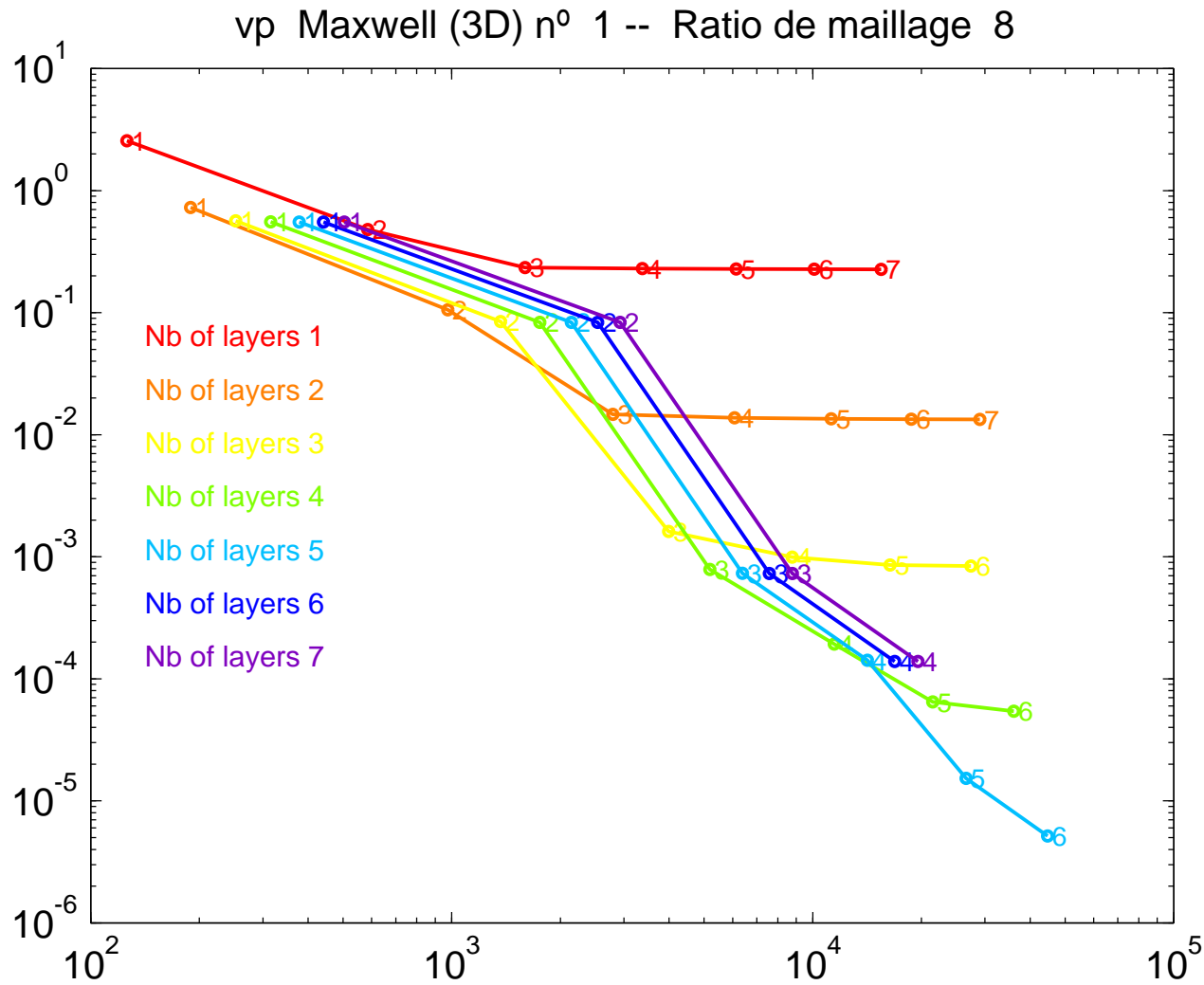
The following 9 graphs show the error as a function of the number of degrees of freedom for the first 8 Maxwell eigenvalues and computed convergence rates for the 4th eigenvalue.

The computations were done for \mathbb{Q}^p elements on a \mathbb{Q}^1 -hexahedral mesh, obtained by using a geometrically refined mesh on L with refinement ratio 8 and a variable number of layers indicated by color, and two layers in the third dimension.

The degree p varies from 1 to 6.

For the weight sr^α , we used $s = 40$, $\alpha = 2$, and r the distance to the singular edge $\{(0, 0)\} \times [0, 1]$.

The Thick L: Maxwell Eigenvalue 1

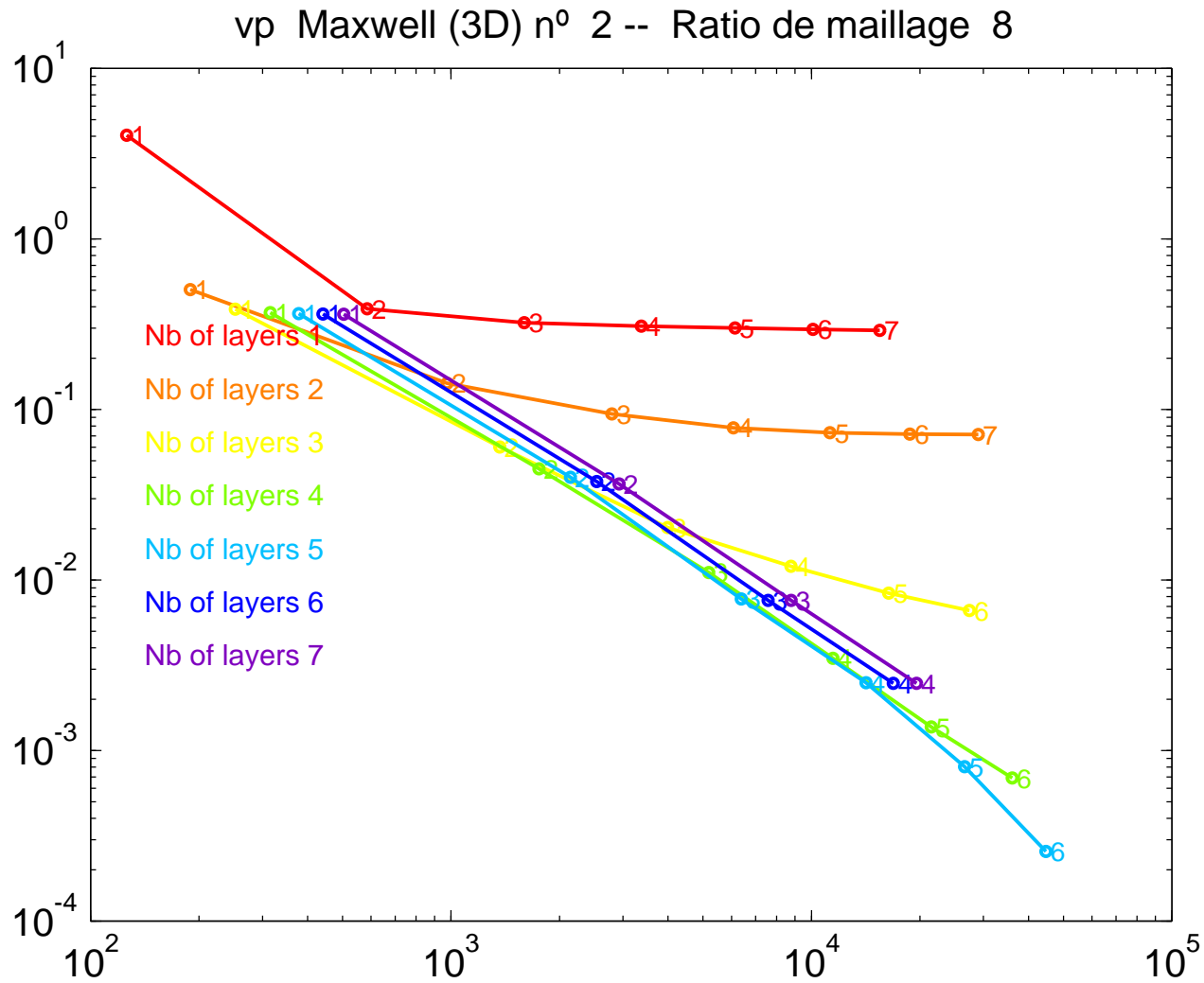


rel. error vs #dof

$$1 \leq p \leq 6$$

$$1 \leq \#layers \leq 7$$

The Thick L: Maxwell Eigenvalue 2

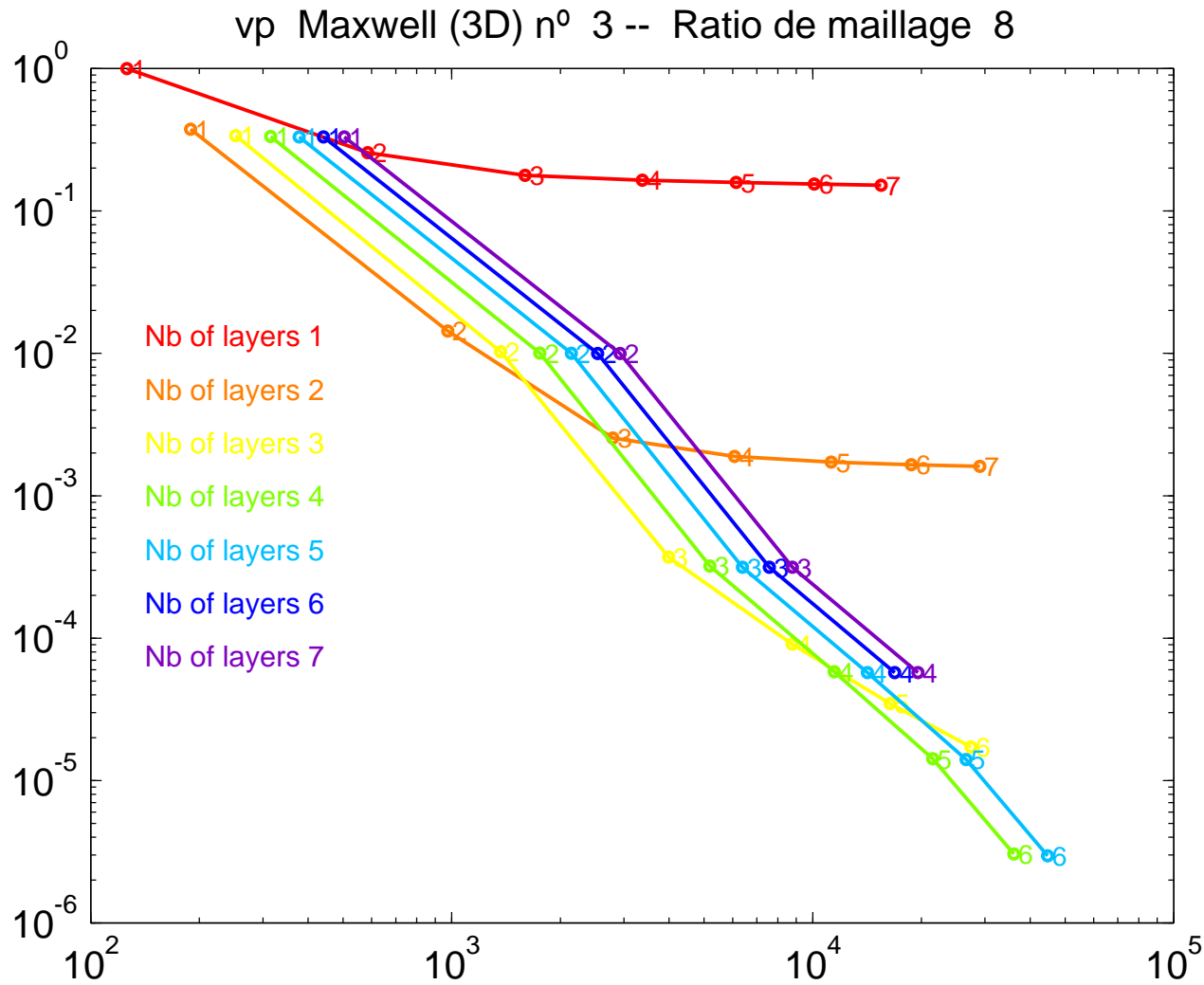


rel. error vs #dof

$$1 \leq p \leq 6$$

$$1 \leq \#layers \leq 7$$

The Thick L: Maxwell Eigenvalue 3

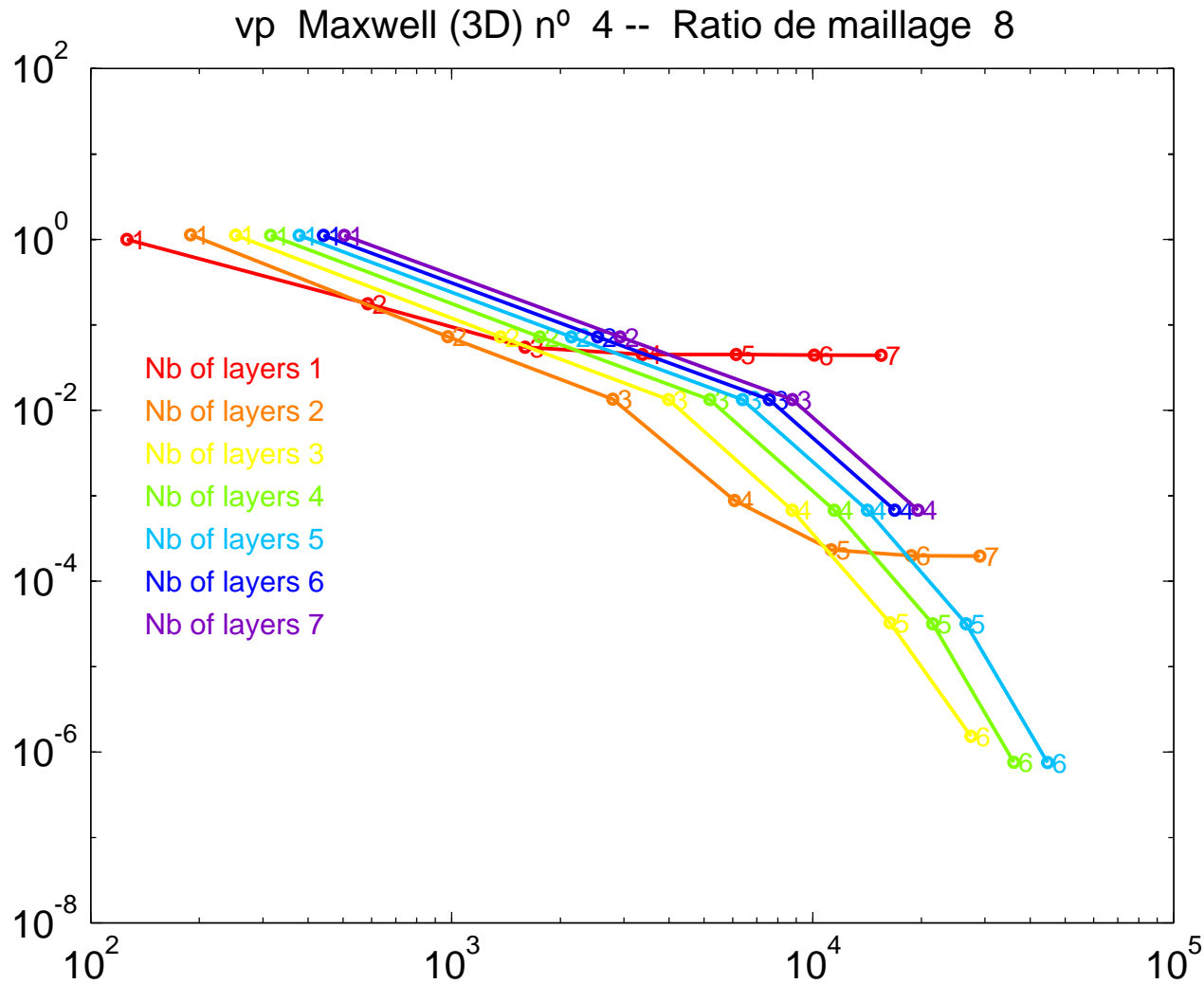


rel. error vs #dof

$$1 \leq p \leq 6$$

$$1 \leq \#layers \leq 7$$

The Thick L: Maxwell Eigenvalue 4

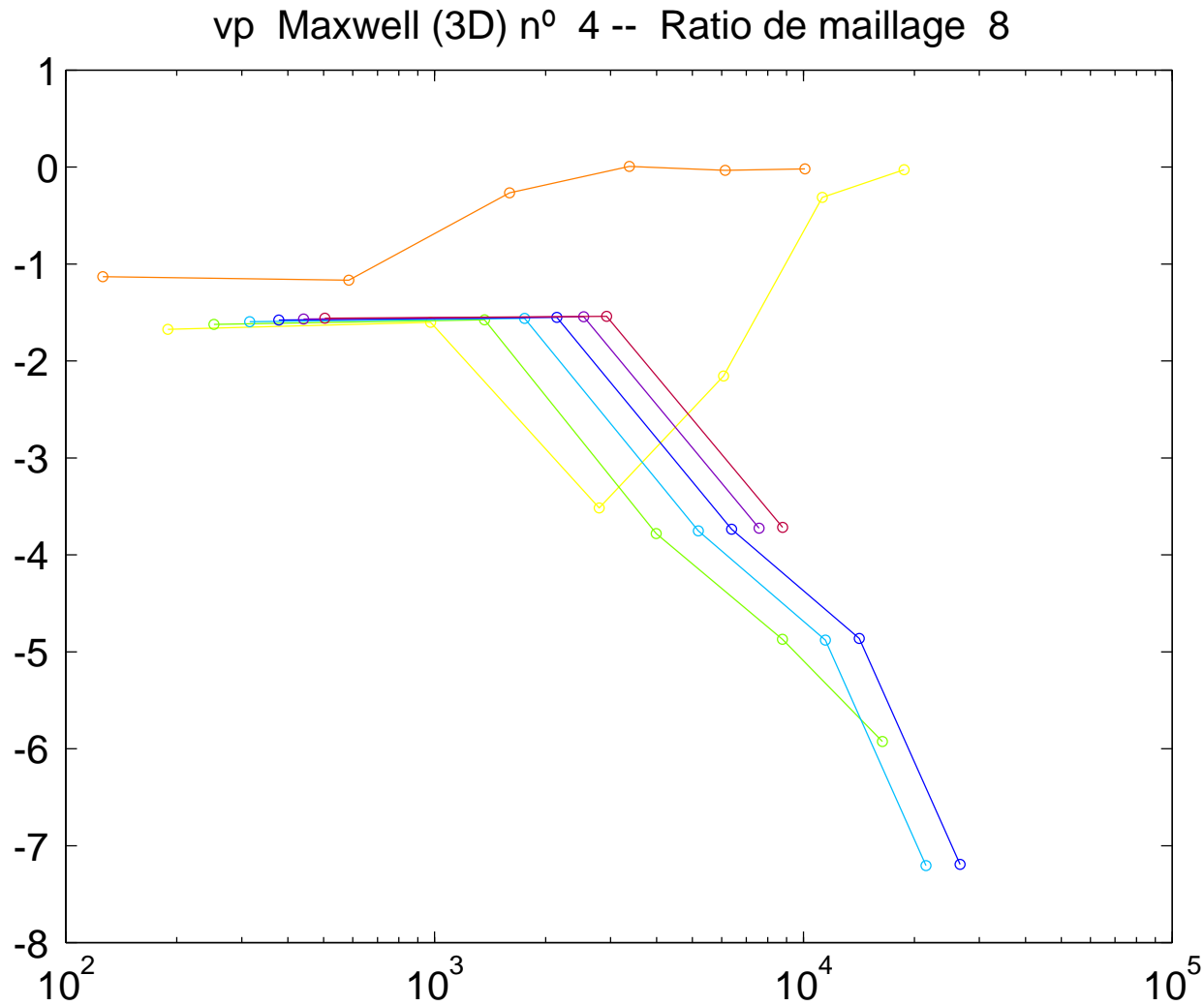


rel. error vs #dof

$$1 \leq p \leq 6$$

$$1 \leq \#layers \leq 7$$

The Thick L: Maxwell Eigenvalue 4

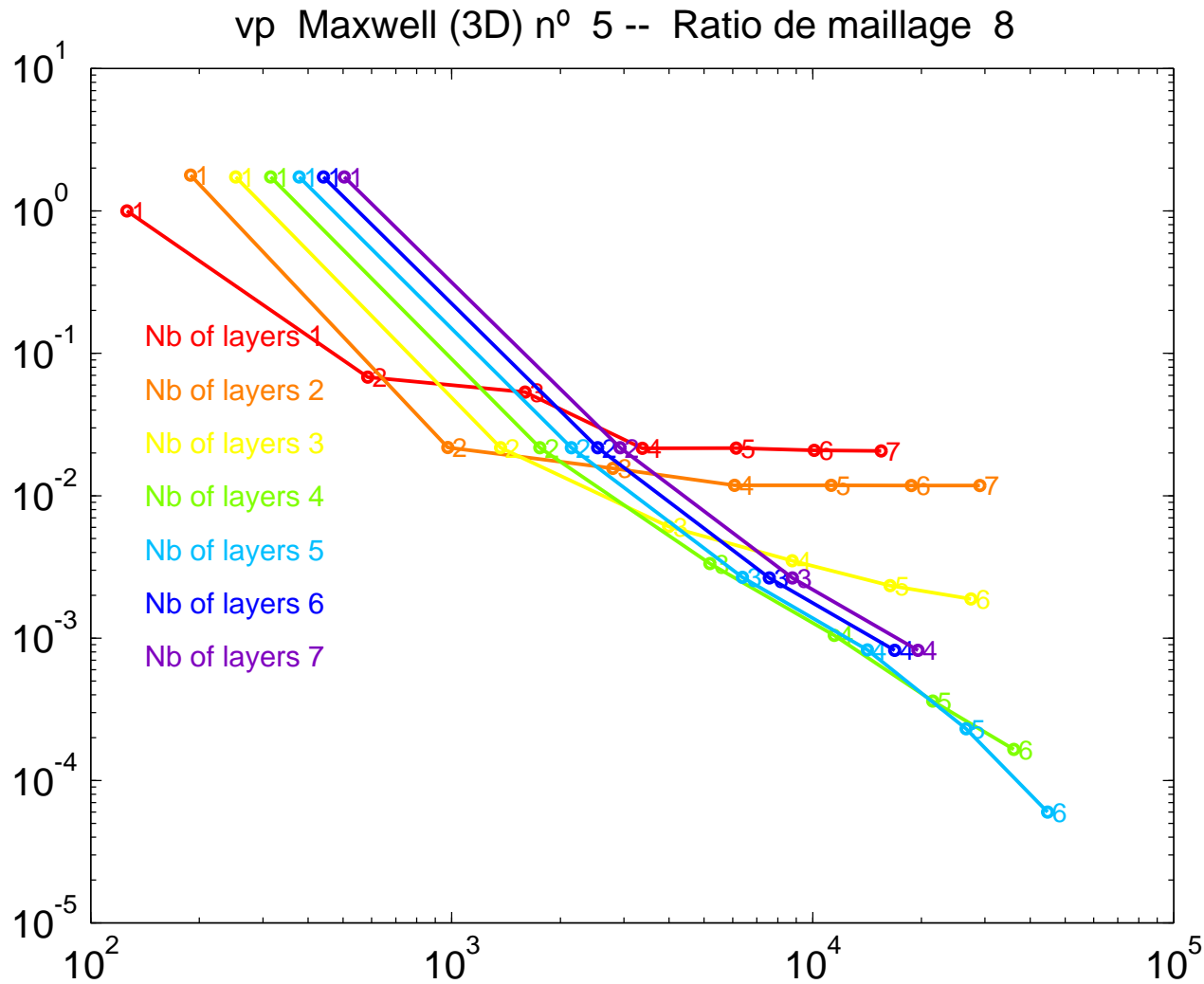


convergence rates

$$1 \leq p \leq 6$$

$$1 \leq \#layers \leq 7$$

The Thick L: Maxwell Eigenvalue 5

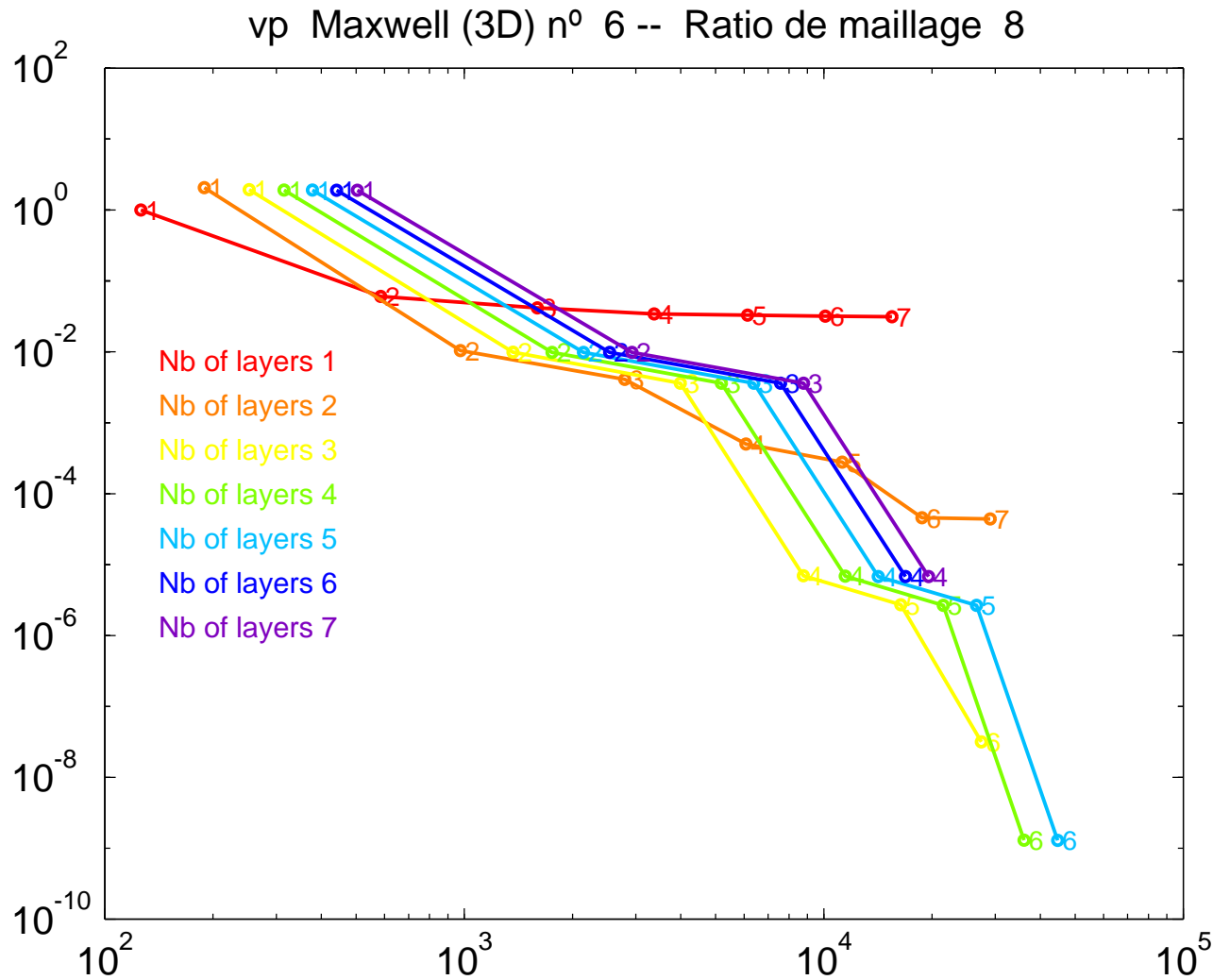


rel. error vs #dof

$$1 \leq p \leq 6$$

$$1 \leq \#layers \leq 7$$

The Thick L: Maxwell Eigenvalue 6

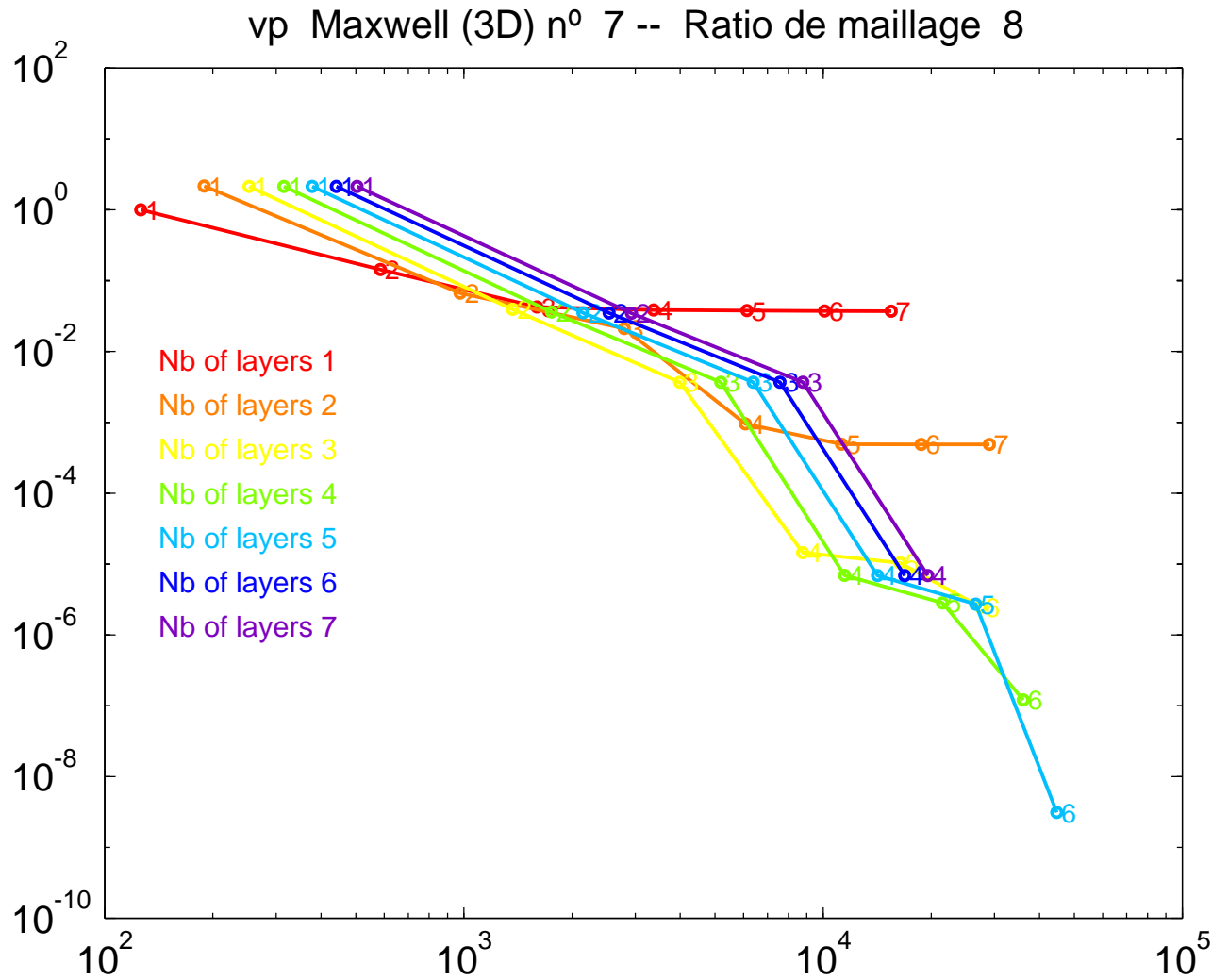


rel. error vs #dof

$$1 \leq p \leq 6$$

$$1 \leq \#layers \leq 7$$

The Thick L: Maxwell Eigenvalue 7

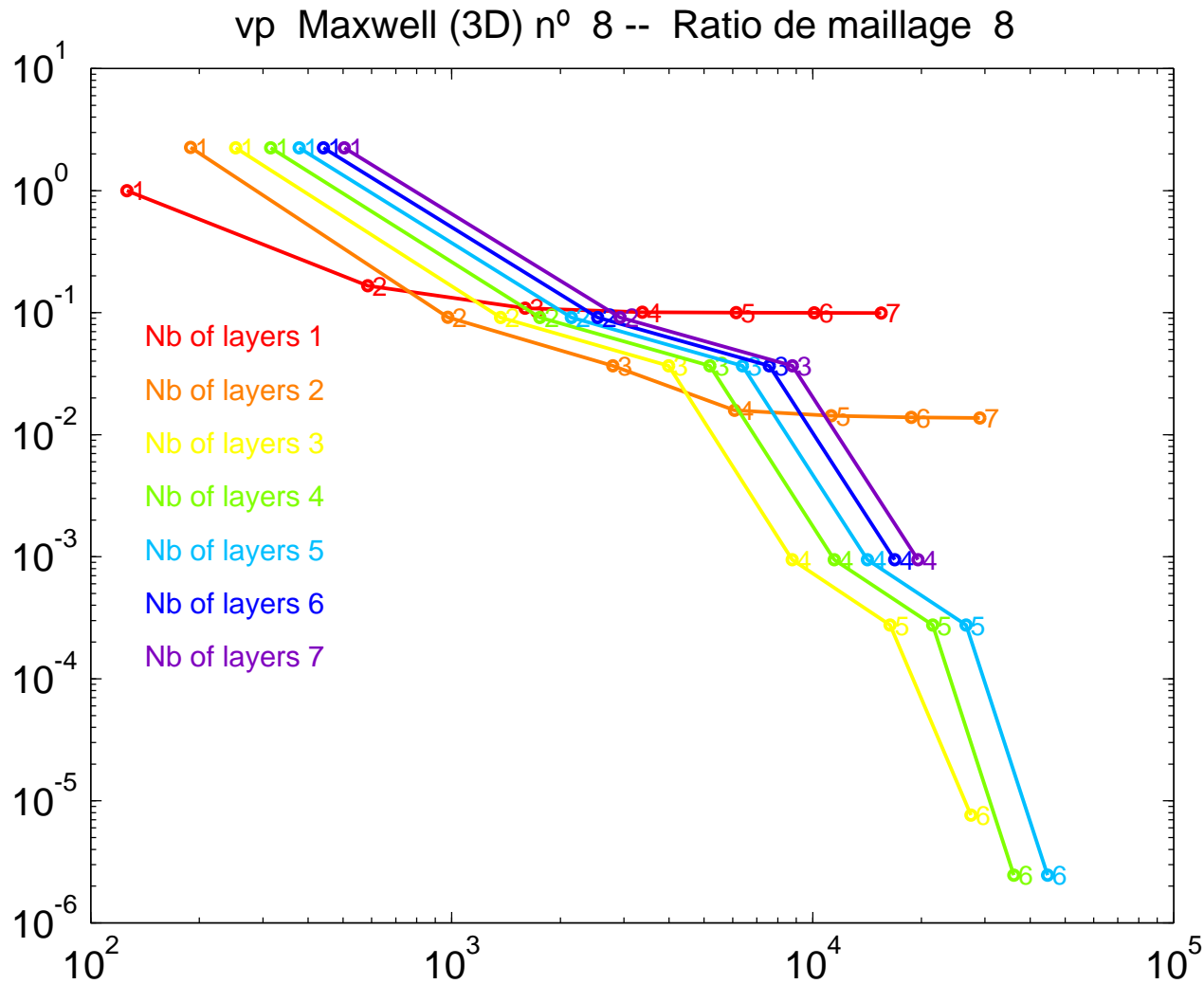


rel. error vs #dof

$$1 \leq p \leq 6$$

$$1 \leq \#layers \leq 7$$

The Thick L: Maxwell Eigenvalue 8



rel. error vs #dof

$$1 \leq p \leq 6$$

$$1 \leq \#layers \leq 7$$

Fichera Corner

The eigenvalues for this domain are not known. Therefore we show the validity of our computations with the weighted regularization method in two ways:

- Dependence of the eigenvalues on the parameter s in the weight sr^α :
We compute the first 20 Maxwell eigenvalues for s ranging from 0 to 20. The curl dominant eigenvalues are shown in blue, the div dominant eigenvalues in red, and the indifferent ones in green (factor $\rho = 1.5$).
We see that for $\alpha = 2$ the eigenvalues show the required behavior, i.e. they lie on two families of straight lines. Without weight ($\alpha = 0$), the behavior is different.
- Approximation of the cube. We deform the 7/8th cube so that it approximates the unit cube $[0, 1]^3$. The Maxwell eigenvalues for the latter are known (π^2 times sums of squares of integers). In our graphs, we show the eigenvalues divided by π^2 to make this approximation more evident.

Fichera Corner cont'd

We show computations for 4 domains:

F_0 , the 7/8th cube $[-1, 1]^3 \setminus [-1, 0]^3$.

The eigenvalues have high multiplicity due to symmetries.

$F_1 = F_0 \cap ([-0.8, 1] \times [-0.5, 1] \times [-1, 1])$

Here the symmetries are broken.

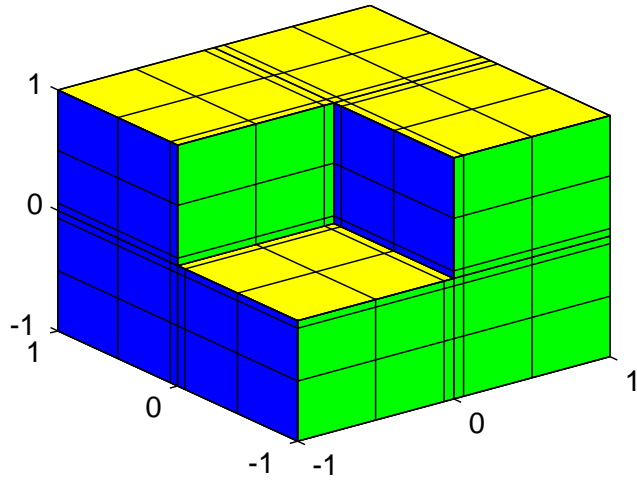
From F_1 to F_2 and from F_2 to F_3 , the thickness of the 6 protruding hexahedra is reduced by a factor of 10, so that F_3 is 1% away from the unit cube $[0, 1]^3$ in Hausdorff distance.

We use \mathbb{Q}^4 hexahedral elements on a tensor product mesh generated from the 1-dimensional mesh $\{0, 1/64, 1/2, 1\} \subset [0, 1]$.

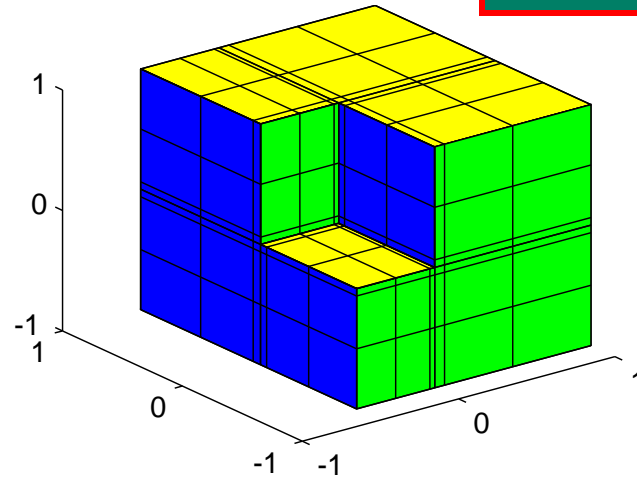
For readability reasons, in the following picture the refinement ratio 1/64 is replaced by 1/16 and the geometric approximation factor 1/10 by 1/5.

The domains $F0 \dots F3$

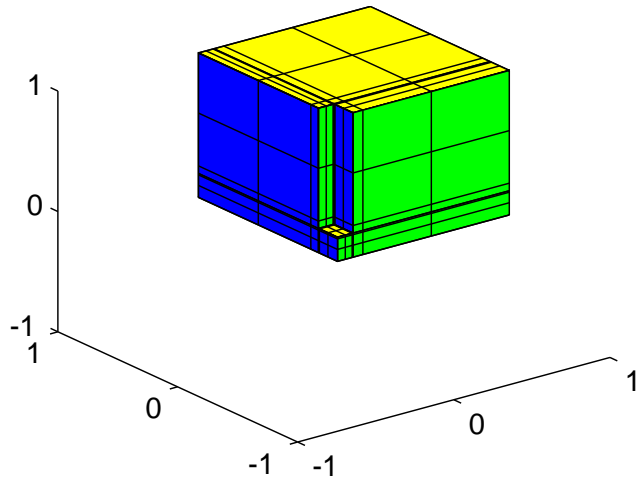
Fichera Corner F0
[a,b,c] = [1,1,1]



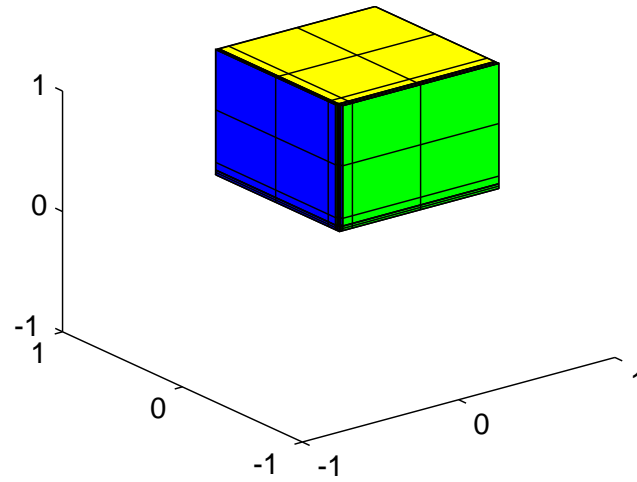
Fichera Corner F1
[a,b,c] = [0.5,0.8,1]



Fichera Corner F2
[a,b,c] = [0.1,0.16,0.2]

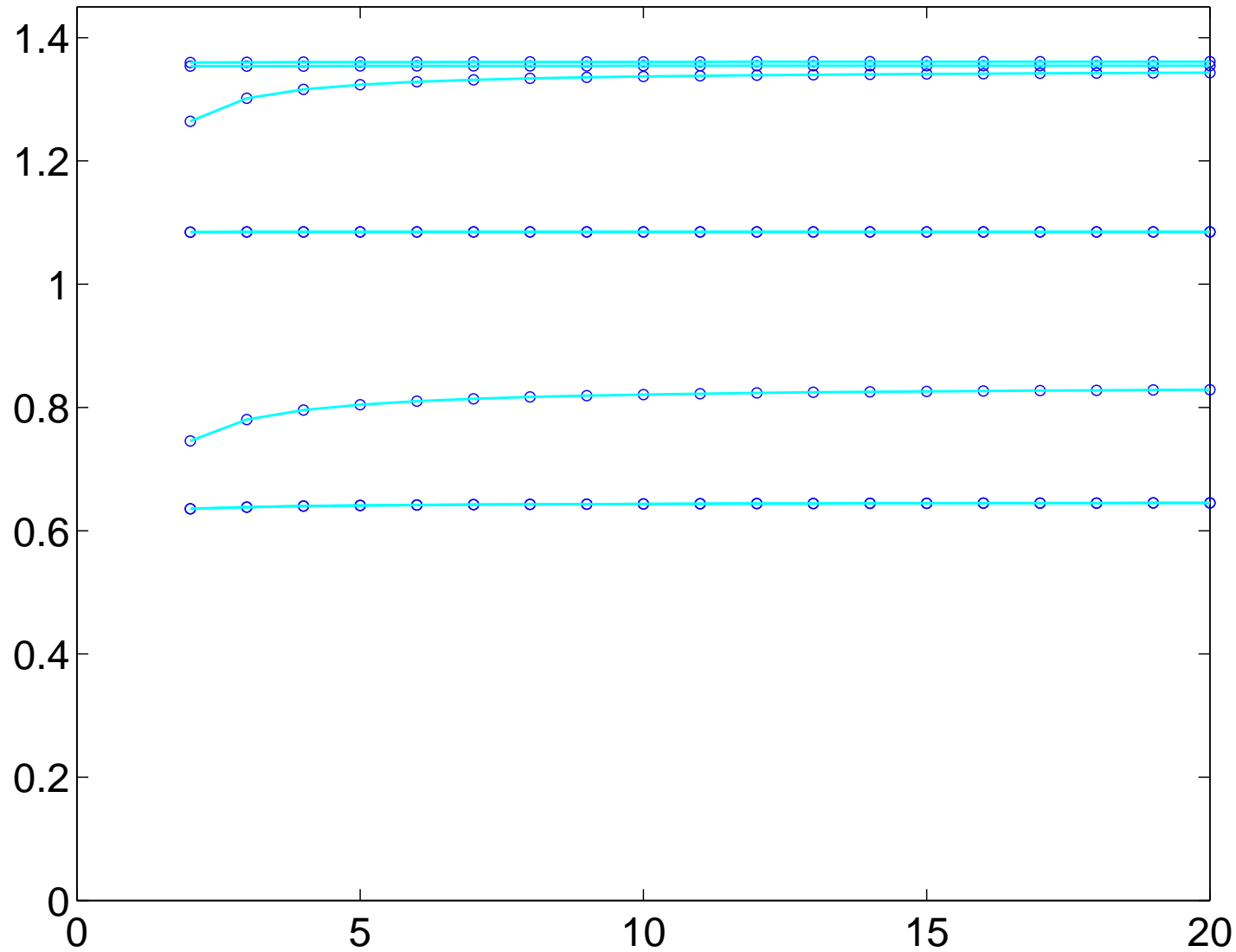


Fichera Corner F3
[a,b,c] = [0.02,0.032,0.04]



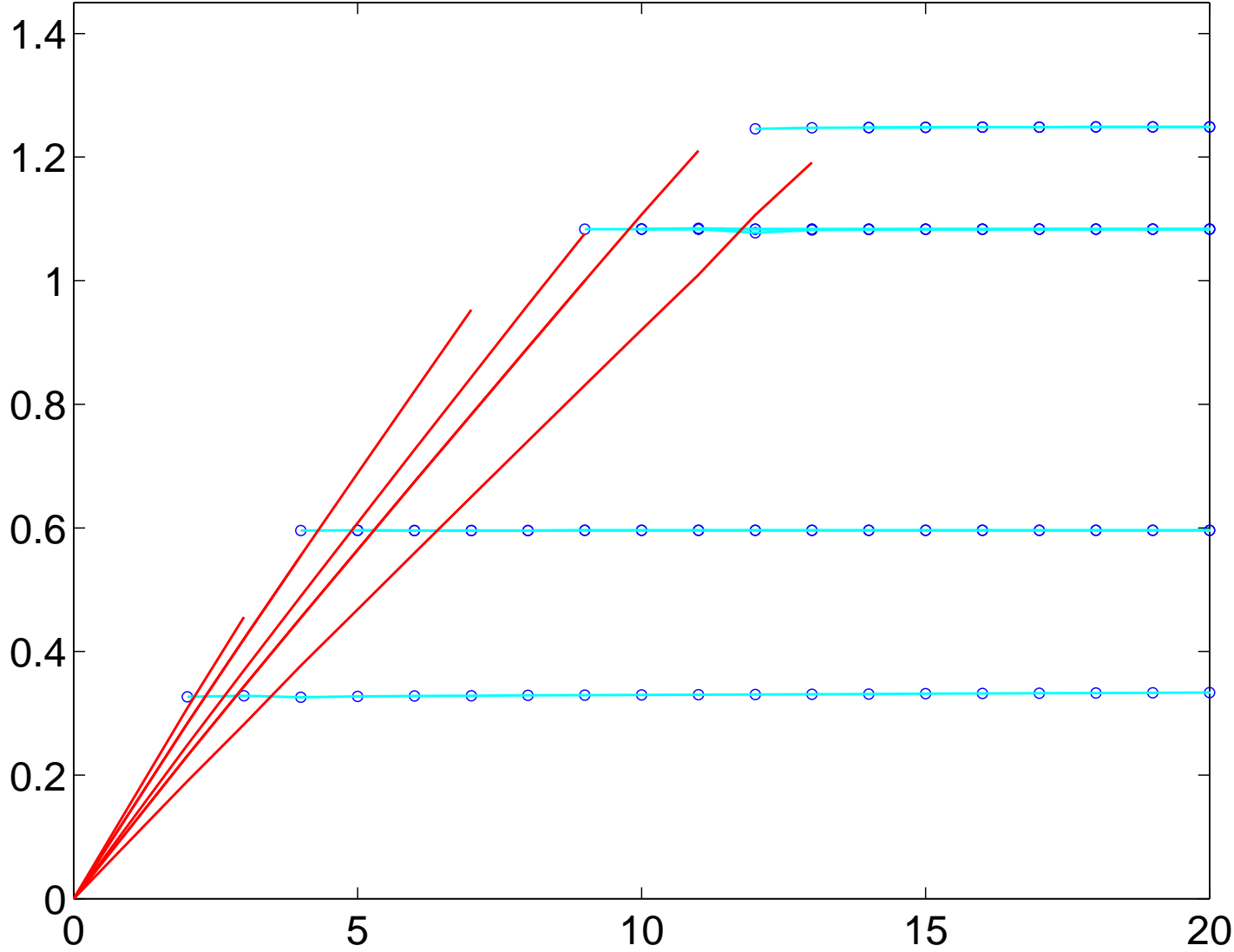
F0, no weight: $\alpha = 0$

Ratio de tri 1.5 et $\alpha = 0$. Domaine F0



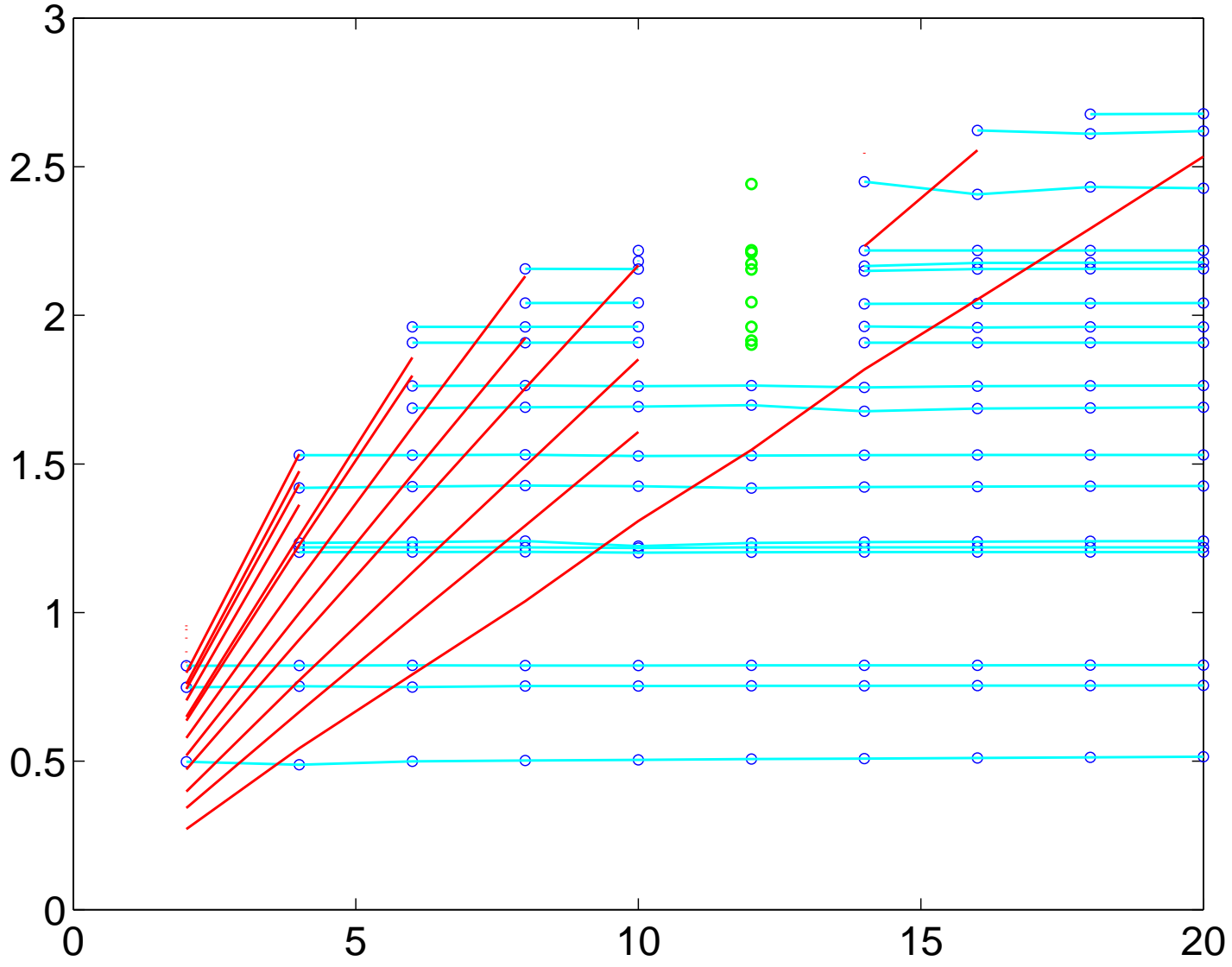
$F0, \alpha = 2$

Ratio de tri 1.5 et $\alpha = 2$. Domaine F0



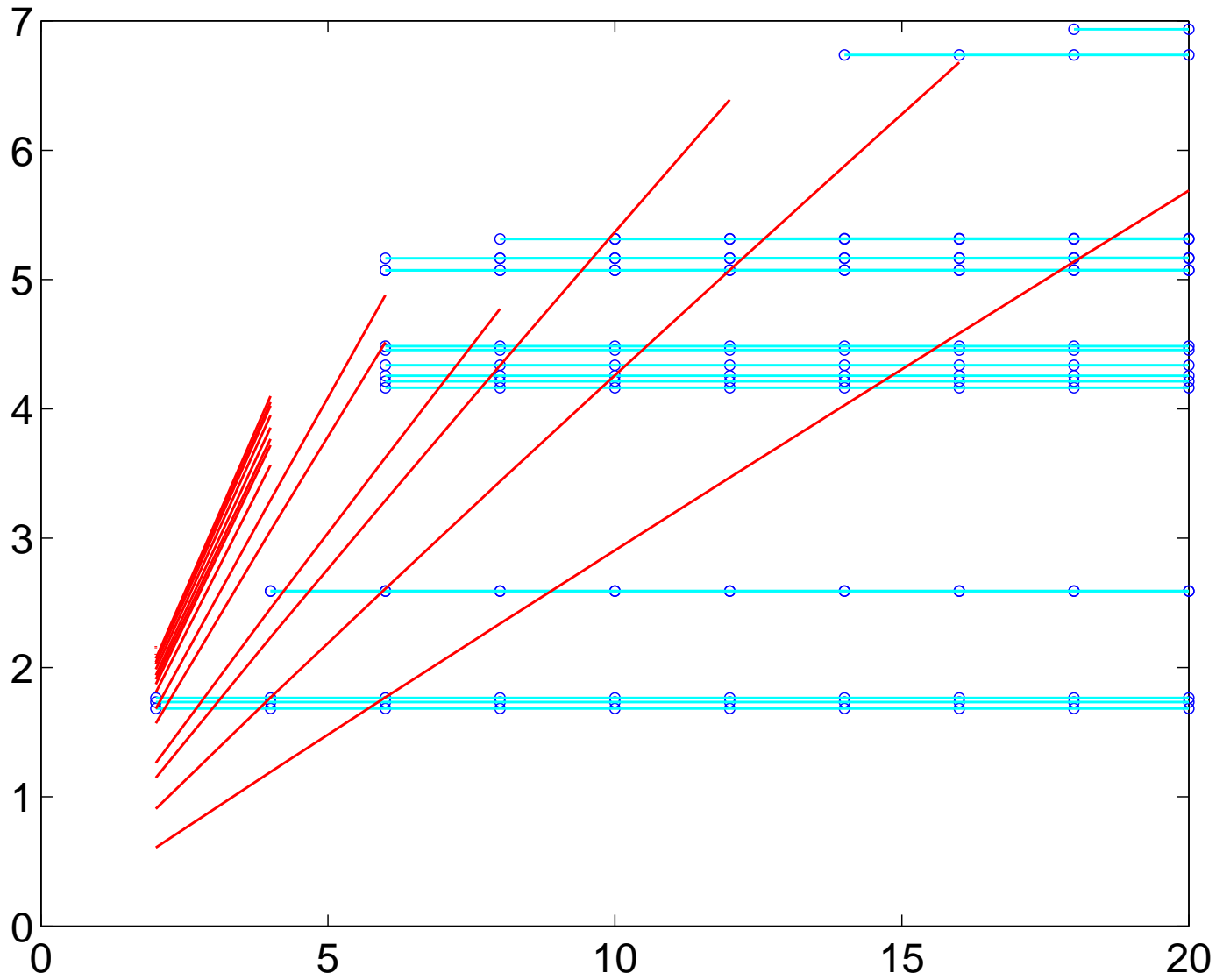
$F1, \alpha = 2$

Ratio de tri 1.5 et $\alpha = 2$. Domaine F1



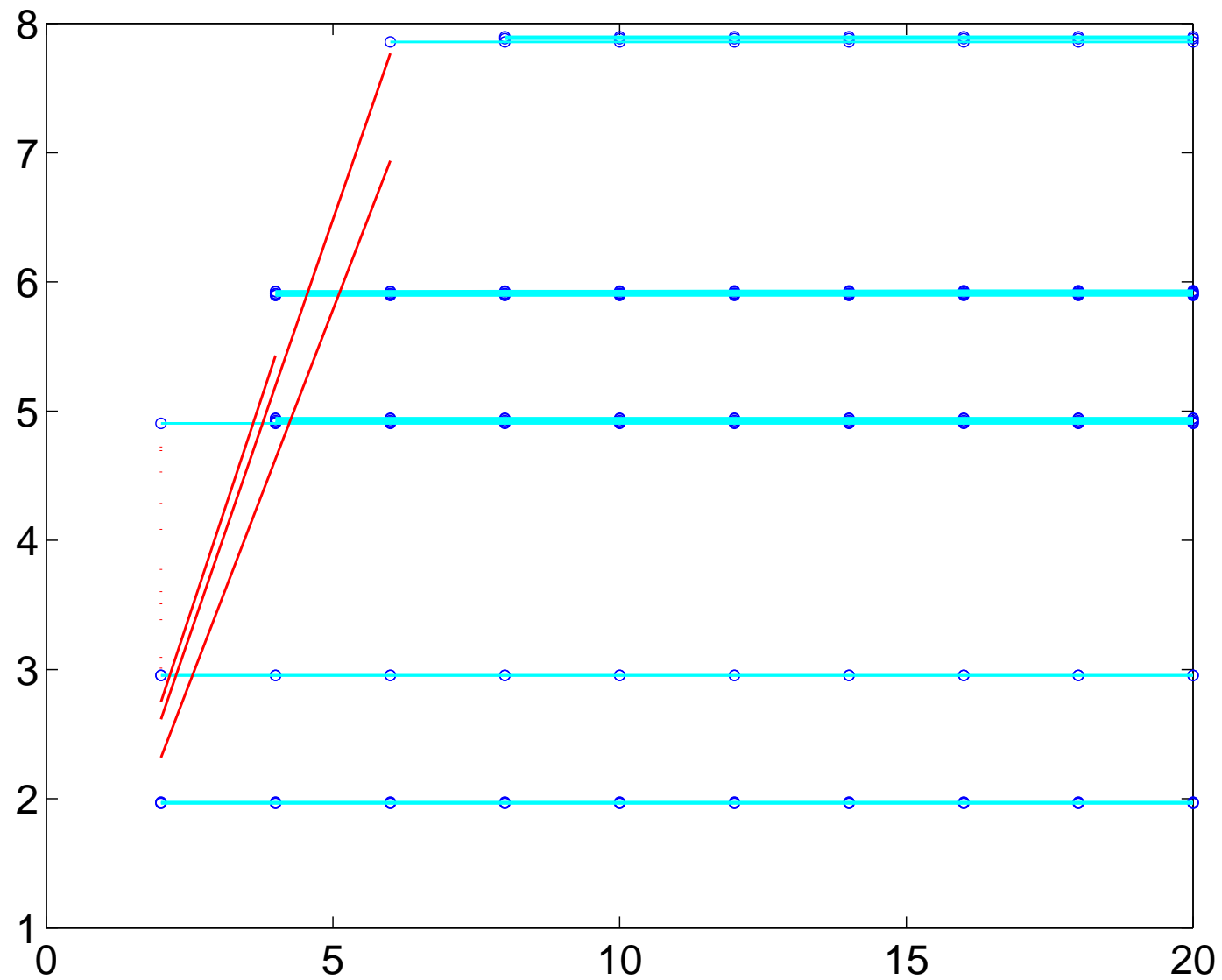
$F2, \alpha = 2$

Ratio de tri 1.5 et $\alpha = 2$. Domaine F2



F3, $\alpha = 2$

Ratio de tri 1.5 et $\alpha = 2$. Domaine F3



Conclusion

The **Weighted Regularization Method** requires only a very simple modification of the standard regularized variational formulation of time-harmonic Maxwell source and eigenvalue problems.

It allows the use of standard nodal finite elements even in the case of domains with reentrant corners and solutions with strong non- H^1 singularities where the standard regularization gives incorrect results.

In combination with the hp version of the finite element method, an efficient and robust algorithm is obtained that allows highly precise approximations even for 3D problems.